

The oldest fossil record of bandicoots (Marsupialia; Peramelemorphia) from the late Oligocene of Australia

K.J. Travouillon, R.M.D. Beck, S.J. Hand, and M. Archer

ABSTRACT

Two new late Oligocene representatives of the marsupial order Peramelemorphia (bandicoots and bilbies) from the Etadunna Formation of South Australia are described here. *Bulungu muirheadae* sp. nov., from Zone B (Ditjimanka Local Fauna [LF]), is represented by several dentaries and isolated upper and lower molars. *Bulungu campbelli* sp. nov., from Zone C (Ngapakaldi LF), is represented by a single dentary and maxilla. Together, they represent the oldest fossil bandicoots described to date. Both are small (estimated body mass of <250 grams) in comparison to most living bandicoot species and were probably insectivorous based on their dental morphology. They appear to be congeneric with *Bulungu palara* from Miocene local faunas of the Riversleigh World Heritage Area (WHA), Queensland and the Kutjamarpu LF (Wipajiri Formation) of South Australia. However, the Zone B peramelemorphian appears to be more plesiomorphic than *B. palara* in its retention of complete centrocristae on all upper molars.

K. J. Travouillon. School of Earth Sciences, University of Queensland, St Lucia, Queensland 4072, Australia kennytravouillon@hotmail.com
and School of Biological, Earth and Environmental Sciences, University of New South Wales, New South Wales 2052, Australia
R.M.D. Beck. School of Biological, Earth and Environmental Sciences, University of New South Wales, New South Wales 2052, Australia robin.beck@unsw.edu.au
S.J. Hand. School of Biological, Earth and Environmental Sciences, University of New South Wales, New South Wales 2052, Australia s.hand@unsw.edu.au
M. Archer. School of Biological, Earth and Environmental Sciences, University of New South Wales, New South Wales 2052, Australia m.archer@unsw.edu.au

Keywords: Peramelemorphian; Oligocene; South Australia; bandicoot; new species; marsupials

INTRODUCTION

The fossil record of bandicoots and bilbies (Marsupialia: Peramelemorphia) remains relatively

poorly known, with only 13 species described to date (excluding Quaternary records of extant species) from sites spanning the late Oligocene to Pleistocene. The only extinct species to have been

PE Article Number: 16.2.13A
Copyright: Palaeontological Association May 2013
Submission: 6 November 2012. Acceptance: 30 January 2013

Travouillon, K.J., Beck, R.M.D., Hand, S.J., and Archer M. 2013. The oldest fossil record of bandicoots (Marsupialia; Peramelemorphia) from the late Oligocene of Australia, *Palaeontologia Electronica* Vol. 16, Issue 2; 13A 52p; palaeo-electronica.org/content/2013/400-late-oligocene-bandicoot

<http://zoobank.org/A47937B6-444F-4BF1-B66A-0ECDE2E6BC27>

described from the Pleistocene is *Perameles sobbei* from the Darling Downs, Queensland (Price, 2002; 2005). Five Pliocene peramelemorphians have been described including *Perameles allinghamensis* from the Bluff Downs Local Fauna (LF), Queensland (Archer and Wade, 1976), *Perameles bowensis* from the Bow and Wellington Caves LFs, New South Wales (Muirhead et al., 1997), cf. *Peroryctes tedfordi* and cf. *Peroryctes* sp. from the Hamilton LF, Victoria (Turnbull et al., 2003) and *Ischnodon australis*, from the Palankarina LF, South Australia (Stirton, 1955). The bizarre, dentally autapomorphic *Numbigilga ernielundeliusi* from the Bluff Downs LF (Beck et al., 2008a) may represent a sixth Pliocene peramelemorphian species.

Ongoing research on fossil peramelemorphians from late Oligocene and early Miocene sites (Muirhead, 1994, 2000; Muirhead and Filan, 1995; Case, 2001; Schwartz, 2006; Travouillon et al., 2010, 2013; Gurovich et al., 2013), particularly relatively complete specimens from the Riversleigh World Heritage Area (WHA), has led to increasingly detailed knowledge of the evolutionary history of Peramelemorphia during this key period. Six species have been described from the Miocene, namely *Yarala burchfieldi* (Muirhead and Filan, 1995; Muirhead, 2000), *Galadi speciosus* (Travouillon et al., 2010), *G. adversus*, *G. grandis*, *G. amplus* (Travouillon et al., 2013) from Riversleigh LFs, and *Bulungu palara* (Gurovich et al., 2013) from multiple LFs at Riversleigh WHA and the Kutjamarpu LF, South Australia. *Yarala kida* (Schwartz, 2006) from the late Oligocene or early Miocene Kangaroo Well LF (see Metzger and Retallack, 2010) is currently the oldest described peramelemorphian. However, Woodburne et al. (1993) and Case (2001) reported a number of peramelemorphian species from the Etadunna and Wipajiri Formations of South Australia, some of which may predate the Kangaroo Well LF (see also Woodburne and Case, 1996, 144, 150-151).

Here we describe two new peramelemorphian species from two of the oldest faunal zones of the Etadunna Formation, the Ditjimanka LF (Faunal Zone B) and Ngapakaldi LF (Faunal Zone C). We assess the phylogenetic relationships of these to other peramelemorphians to shed light on the early evolutionary history of the order.

MATERIALS AND METHODS

Collecting and Processing

Specimens described here were collected from Tedford Locality (Site 2), site code RV 7230, Lake Palankarina, Etadunna Formation, Ditjimanka LF, Zone B and Ngapakaldi Quarry, site code V 5858, Lake Ngapakaldi, Etadunna Formation, Ngapakaldi LF, Zone C, by Stirton, Tedford, Woodburne, Archer and co-workers between 1957 and 1972. All specimens collected after 1970 were recovered by screen-washing in the field (Campbell, 1976).

Anatomical Terminology

Dental terminology follows Archer (1976), Muirhead and Filan (1995), Travouillon et al. (2010) and Turnbull et al. (2003), with molar loci homology following Lockett (1993). Peramelemorphian systematics follows Muirhead (1994, 2000), Muirhead and Filan (1995) and Travouillon et al. (2010). Higher-level marsupial systematics follow the classification of Aplin and Archer (1987).

Institutional Abbreviations

QM F Queensland Museum Fossil collection, Brisbane, Australia; **SAM P** South Australian Museum, Palaeontology Collection, Adelaide, Australia; **UCMP** University of California, Museum of Paleontology, Berkeley, USA; **UCR** University of California, Riverside, USA.

Body Mass Estimates

The maximum length and width of each tooth on each specimen were measured (see Tables 1 and 2). These measurements were used to estimate individual body mass of each specimen, using Myers' (2001) allometric relationships between dental measurements and body mass for predicting marsupial body mass. We used the highest ranked equation from Myers (2001) in the "all species excluding dasyuromorphians" dataset, which is the most suitable dataset for bandicoots. For example, when more than one tooth was present in a specimen, we used the highest ranked equation on the tooth row (e.g., 4LMA > 3LMA > 2LMA > 1LMA). All body mass estimates are shown in grams in Tables 1 and 2. Average body mass for the species was calculated from these estimates.

Phylogenetic Analysis

Phylogenetic relationships within Peramelemorphia were assessed using a revised ver-

TABLE 1. Measurements of the upper dentition of type and referred material in mm; body mass estimates in grams. L – anteroposterior length, W = lingual-buccal width, M = molar. Measurements of damaged/broken teeth are in brackets.

Taxa	Specimen	Locality	M1		M2		M3		Body mass estimate
			L	W	L	W	L	W	
<i>Bulungu muirheadae</i>	QM F10662	Tedford Locality					2.21	2.12	211.45
<i>Bulungu muirheadae</i>	QM F10664	Tedford Locality			2.22	1.57			129.49
<i>Bulungu muirheadae</i>	QM F10665	Tedford Locality					1.88	1.83	131.95
<i>Bulungu muirheadae</i>	QM F12416	Tedford Locality	2.12	1.84					171.8
<i>Bulungu muirheadae</i>	QM F12417	Tedford Locality					2.05	1.86	154.38
<i>Bulungu muirheadae</i>	QM F12420	Tedford Locality			1.88	1.47			90
<i>Bulungu muirheadae</i>	UCMP 108063	Tedford Locality					2.12	1.98	178.78
<i>Bulungu muirheadae</i>	UCR 15270	Tedford Locality					2.08	1.7	137.59
<i>Bulungu muirheadae</i>	UCR 15275	Tedford Locality					1.89	1.76	125.32
<i>Bulungu muirheadae</i>	UCR 15285	Tedford Locality					2	1.75	135.45
<i>Bulungu muirheadae</i>	UCR 15299	Tedford Locality			1.86	1.45			86.62
<i>Bulungu muirheadae</i>	UCR 15307	Tedford Locality	1.91	1.5					106.22
<i>Bulungu muirheadae</i>	UCR15332	Tedford Locality			(1.83)	1.57			n/a
<i>Bulungu muirheadae</i>	UCR 16996	Tedford Locality	1.88	(1.24)					n/a
<i>Bulungu campbelli</i>	SAM P13853	Ngapakaldi Quarry					1.7	1.75	105.68

sion of the matrix used by Travouillon et al. (2010), Travouillon et al. (2013), and Gurovich et al. (2013), comprising 156 qualitative morphological characters, of which 123 are dental and 33 cranial (see Appendix 1 and 2). To help resolve relationships among fossil peramelemorphians, most of which are known only from isolated dental remains, we have added 96 new dental and cranial characters relative to previous iterations of this matrix. Some characters from the original matrix were modified by adding, removing, or revising ambiguous character states, and some characters were deleted to be replaced by more comprehensive characters (see Appendix 1). Seventy-one characters represent putative morphocline/transformation series (see Appendix 1) and so were ordered in all analyses. All taxa were rescored for this study, to confirm previous scoring decisions and to correct

errors present in previous versions of the matrix (e.g., we revised a number of characters scorings for *Ischnodon australis*). We used the same ingroup peramelemorphian species used by Travouillon et al. (2013) and Gurovich et al. (2013), except as follows. We deleted *Microperoryctes ornata* from the matrix because the specimens from the Australian Museum that were previously (ibid) used to score this taxon have subsequently been reassigned by museum staff to *Microperoryctes longicauda*. We have also scored and added all fossil bandicoots described to date to the matrix (cf. *Peroryctes tedfordi*, cf. *Peroryctes* sp., *Perameles sobbei*, *Perameles bowensis*, *Perameles allinghamensis*, *Ischnodon australis*, *Yarala burchfieldi*, *Yarala kida*, *Galadi speciosus*, *Galadi grandis*, *Galadi amplius*, *Galadi adversus* and *Bulungu palara*). *Numbigilga ernielundeliusi*

TABLE 2. Measurements of the lower dentition of type and referred material in mms; body mass estimates in grams. L = anteroposterior length, AW = anterior width, PW = posterior width, m = molar.

Taxa	Specimen	Locality	m1		m2		m3		m4		Body mass estimate
			L	W	L	W	L	W	L	W	
<i>Bulungu muirheadae</i>	QM F10661	Tedford Locality	1.57	1.12							109.34
<i>Bulungu muirheadae</i>	QM F10666	Tedford Locality	1.71	1	1.84	1.14	1.95	1.19			127.57
<i>Bulungu muirheadae</i>	QM F10667	Tedford Locality			1.67	1.25	1.89	1.26	-	1.02	132.31
<i>Bulungu muirheadae</i>	QM F10668	Tedford Locality							2.17	1.17	186.66
<i>Bulungu muirheadae</i>	QM F10669	Tedford Locality	1.7	1.09	1.76	1.24					118.22
<i>Bulungu muirheadae</i>	QM F12414	Tedford Locality					1.9	1.23			128.85
<i>Bulungu muirheadae</i>	QM F12415	Tedford Locality					2.17	1.38			182.68
<i>Bulungu muirheadae</i>	QM F12418	Tedford Locality					2.1	1.28			156.9
<i>Bulungu muirheadae</i>	QM F12419	Tedford Locality	1.73	1.15							124.59
<i>Bulungu muirheadae</i>	UCR 15266	Tedford Locality							2	1.03	142.1
<i>Bulungu muirheadae</i>	UCR 15268	Tedford Locality	1.91	1.17							147.14
<i>Bulungu muirheadae</i>	UCR 15279	Tedford Locality			1.79	1.12					104.66
<i>Bulungu muirheadae</i>	UCR 15301	Tedford Locality			1.76	1.18					110.1
<i>Bulungu muirheadae</i>	UCR 15306	Tedford Locality					1.89	1.21			124.97
<i>Bulungu muirheadae</i>	UCR 15318	Tedford Locality			1.78	1.24					120.16
<i>Bulungu muirheadae</i>	UCR 17002	Tedford Locality					2.2	1.5			209.44
<i>Bulungu campbelli</i>	SAMP 13853	Ngapakaldi Quarry			1.79	1.11	1.75	1.32	1.79	1.09	132.38
<i>Bulungu campbelli</i>	SAMP 13853	Ngapakaldi Quarry	1.55	1.07							100.56

has not been included, due to its highly autapomorphic dental morphology and questionable peramelemorphian affinities. In addition to the outgroup taxa used by Travouillon et al. (2013) and Gurovich et al. (2013) – namely the fossil dasyuromorphians *Barinya wangala* and *Mutpuracinus archibaldi* and the early Eocene stem-australidelphan *Djarthia murgonensis*, we also scored five new extant outgroup species from the family Dasyuridae: the dasyurines *Dasyurus hallucatus*, *Dasyuroides byrnei*, *Phascogale tapoatafa* and

Antechinus stuartii, and the sminthopsine *Sminthopsis macroura*.

Unconstrained Maximum Parsimony Analysis

Unconstrained maximum parsimony analysis of the matrix was performed using PAUP* 4.0b10 (Swofford, 2002). Following Worthy et al. (2006) and Beck et al. (2008b), a two-stage search strategy was used with an initial search comprising 1,000 heuristic replicates, saving 10 trees per replicate, followed by a second heuristic search within

these saved trees. The multiple most parsimonious trees produced were summarised using strict consensus. Bootstrap values for each node in the strict consensus were calculated using 1000 bootstrap replicates, each of which itself comprises 10 random addition replicates. Decay indices were also calculated using AutoDecay 5.0 (Eriksson, 2001) in combination with the perl script perlRat, which implements the parsimony ratchet; the default settings for perlRat (five batches of 200 replicates, randomly upweighting 25% of characters by a factor of two) were used to implement parsimony ratchet searches to calculate decay indices for all nodes in the strict consensus.

Molecular Scaffold Parsimony Analysis

For this analysis, the matrix was analysed using the same methods as for the unconstrained maximum parsimony analysis, but with a “molecular scaffold” as a “backbone” constraint. For the molecular scaffold, relationships among extant peramelemorphians were constrained to match the recent molecular phylogeny of Westerman et al. (2012); only those peramelemorphian taxa analysed by Westerman et al. (2012) were included in the molecular scaffold, and only those clades that received $\geq 70\%$ partitioned maximum likelihood bootstrap support and ≥ 0.95 partitioned Bayesian posterior probability in the analyses of Westerman et al. (2012, table 2) were enforced as monophyletic. The five extant dasyurid outgroup taxa were also included in the molecular scaffold, with their relationships constrained to match those recovered by Krajewski et al. (2007, figure 5) and Westerman et al. (2008, figure 2). As in the unconstrained maximum parsimony analysis, bootstrap support values were calculated for all nodes present in the strict consensus of most parsimonious trees and using 1000 bootstrap replicates of 10 random addition sequence replicates each, but enforcing the molecular scaffold. The molecular scaffold topology is included in the supplementary information accompanying this paper (Appendix 3).

Unconstrained Bayesian Analysis

Bayesian analysis of the matrix using the Lewis (2001) “Mk” model for discrete morphological characters was implemented with MrBayes 3.2. Because the matrix included autapomorphies, the analysis assumed that variable (rather than purely parsimony-informative) characters were scored (“coding=var”). The analysis was run for 5 million generations but with otherwise default settings. The first 1.25 million generations (i.e., 25%) were

discarded as burn-in. The potential scale reduction factor (PSRF) and minimum and average effective sample sizes (ESS) for both the tree length and alpha parameters were 1.0 and >5000 , respectively, for the post-burn-in trees, indicating that stationarity and convergence had been achieved. The post-burn-in trees were summarised using 50% majority rule consensus, with Bayesian posterior probabilities as support values.

Molecular Scaffold Bayesian Analysis

The Bayesian analysis was repeated enforcing the same molecular scaffold as for the molecular scaffold parsimony analysis. The molecular scaffold was implemented using multiple “partial” constraints, with each constraint corresponding to a node in the molecular scaffold. All other settings were the same as for the unconstrained Bayesian analysis. The potential scale reduction factor (PSRF) and minimum and average effective sample sizes (ESS) for both the tree length and alpha parameters were 1.0 and >5000 , respectively, for the post-burn-in trees, indicating that stationarity and convergence had been achieved.

SYSTEMATIC PALEONTOLOGY

Order: PERAMELEMORPHIA (Kirsch, 1968) Aplin and Archer, 1987

Superfamily: *Incertae sedis*

Family: *Incertae sedis*

Genus: *BULUNGU* Gurovich et al., 2013

Type Species. - *Bulungu palara* Gurovich et al., 2013

Revised Generic Diagnosis

The species of *Bulungu* are small peramelemorphians (estimated body mass of ~110-210 grams) that differ from all others in the following combination of features: M3 preprotocrista terminates at the lingual base of paracone, resulting in an incomplete anterior cingulum on M3; posterior cingulum absent on M3; stylar cusp B (StB) on M3 large and oval with a crest present, but this crest does not connect to StD; StC present as a small cusp on M3 but StD1 is absent; metaconule small and never as lingually positioned as protocone (hence molars subtriangular rather than quadrilateral in occlusal outline); preentocristid anteroposteriorly-orientated on m1-4; no cuspids exist within hypoflexid region between talonid and trigonid on buccal side but a small shelf is present on m1-4; cristid obliqua contacts trigonid buccal to protoconid on m1, just lingual to protoconid on m3 and lingual to midpoint of metacristid on m4; paraconid-

metaconid distance shorter than metaconid-protocoid distance in m2-3 but longer in m4; entoconid large on m4; posthypocristid oblique to tooth row axis on m2 but perpendicular on m3; talonid reduced on m4; molar crowns are distinct from roots.

The following combination of features seen in *Bulungu palara* may also be generically diagnostic, but is as yet unknown for other species in this genus (as they are currently known only from dental specimens): small canines; nasals extend posteriorly past anterior margin of orbit; two pairs of large palatal fenestrae present in palate posterior to incisive foramina; alisphenoid and parietal in contact on lateral wall of braincase (squamosal-frontal contact absent); sphenorbital fissure and foramen rotundum elongate and tube-like, not opening directly into endocranial cavity; primary foramen ovale very large and between petrosal and alisphenoid; bulbous alisphenoid tympanic wings cover anterolateral and medial sides of auditory recess; rostral tympanic process of petrosal an elongate ridge extending length of promontorium but without forming a hypotympanic sinus; epitympanic recess relatively shallow; an arch is formed by paroccipital and mastoid processes, through which is exposed part of the petrosal immediately posterior to fenestra cochleae; rim of postglenoid foramen formed almost exclusively by squamosal with only small contribution from petrosal; in posterior view, occiput is wider than high.

BULUNGU MUIRHEADAE, sp. nov.

Figures 1–2

<http://zoobank.org/F7059F8F-F295-4AD2-9084-54874CF57076>

Specific Diagnosis

Bulungu muirheadae differs from *Bulungu palara* in the following combination of features: postparacrista and premetacrista contact each other, forming a complete centrocrista on M1-3; StC large on M1 (sometimes larger than StB); StD1 larger and distinct on M1 and M2; metaconule smaller and positioned more buccally on M1-3; preparacrista connects to StB on M2, but ends at the base of StA on M3; StE is a distinct cusp on M3; anterior cingulid present on m1; cristid obliqua terminates posterior to protoconid on m2; short postentocristid present on m4, and runs anteroposteriorly; posthypocristid is oblique to the tooth row axis on m4; hypoconulid present as small cusp on m4.

Specific Etymology

The species name honours vertebrate palaeontologist Jeanette Muirhead for her contribution to our understanding of fossil bandicoot taxonomy and evolution.

Holotype

QM F10666, left dentary with m1-3 (Figure 1).

Paratypes

QM F10668, left dentary fragment with m4 (Figure 1); QM F10669, right dentary fragment with m1-2 (Figure 1); UCR 15307, LM1 (Figure 2); QM F10664, LM2 (Figure 2); and UCR 15275, RM3 (Figure 2).

Referred Material

QM F10661, Rm1; QM F10662, RM3; QM F10665, RM3; QM F10667, right dentary with m2-3 and trigonid of m4; QM F12414, Rm3; QM F12415, Lm3; QM F12416, RM1; QM F12417, LM3; QM F12418, Lm3; QM F12419, Lm1; QM F12420, RM2; UCMP 108063, left maxilla fragment with M3; UCR 15266, Rm4; UCR 15268, Rm1; UCR 15270, LM3; UCR 15279, Lm2; UCR 15285, LM3; UCR 15299, RM2; UCR 15301, Lm2; UCR 15306, Rm3; UCR 15318, Lm2; UCR 15332, RM2; UCR 16996, LM1; UCR 17002, Lm3.

Type Locality

Tedford Locality (Site 2), site code RV 7230, Lake Palankarina, Etadunna Formation, Ditjimanka LF, Zone B.

Age and Stratigraphy

The Ditjimanka LF lies within Etadunna Faunal Zone B. Based on palaeomagnetic and drill-core data, Metzger and Retallack (2010) estimated the Etadunna Formation to span 26.1 to 23.6 m.y.a. The Ditjimanka LF is therefore late Oligocene in age.

DESCRIPTION

Dentary

Alveolar margin of the dentary increases in height from p1 to p3, decreases below m1, and then increases again from m2 to m4 (Figure 1). Depth of ramus greatest below m4. Two short subequal diastemata present: first between the alveoli for c1 and p3; second between alveoli for p1 and p2. The symphysis extends as far as posterior alveolus for p2. Two mental foramina present. Anterior of these two is below diastema between

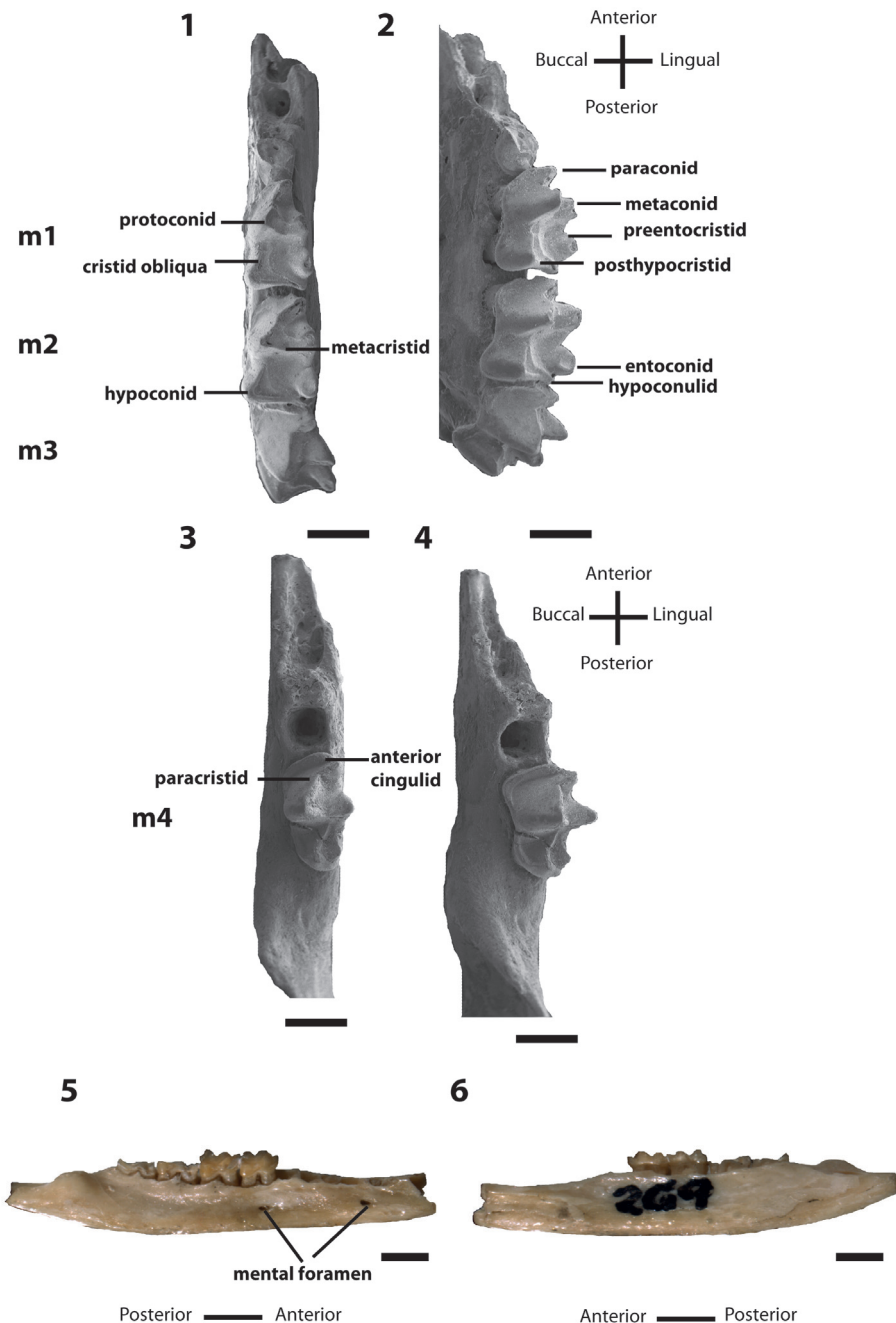


FIGURE 1. *Bulungu muirheadae*, sp. nov. Holotype QM F10666, **1**, occlusal view of left dentary; **2**, buccal view of left dentary. Paratype QM F10668, **3**, occlusal view of left dentary; **4**, buccal view of left dentary. Paratype QM F10669, **5**, buccal view of right dentary; **6**, lingual view of right dentary. Scale bars for **1-4** equals 1mm, for **5-6** equals 2mm.

alveoli for p1 and p2; posterior foramen is below anterior alveolus for m1. Coronoid process forms an angle with body of dentary of approximately 120 degrees.

Lower Dentition

The description of p3 and m1 to m3 is based on QM F10666; that of m4 is based on QM F10668

(Figure 1). Only posterior part of p3 is preserved. The posterior cusp is low and obscured by paraconid of m1. Posterior width of p3 narrower than trigonid of m1.

Protoconid and metaconid of m1 closer together than either is to paraconid. Protoconid tallest cusp on crown, followed by entoconid, metaconid, paraconid, hypoconid, and hypoconulid. A thin

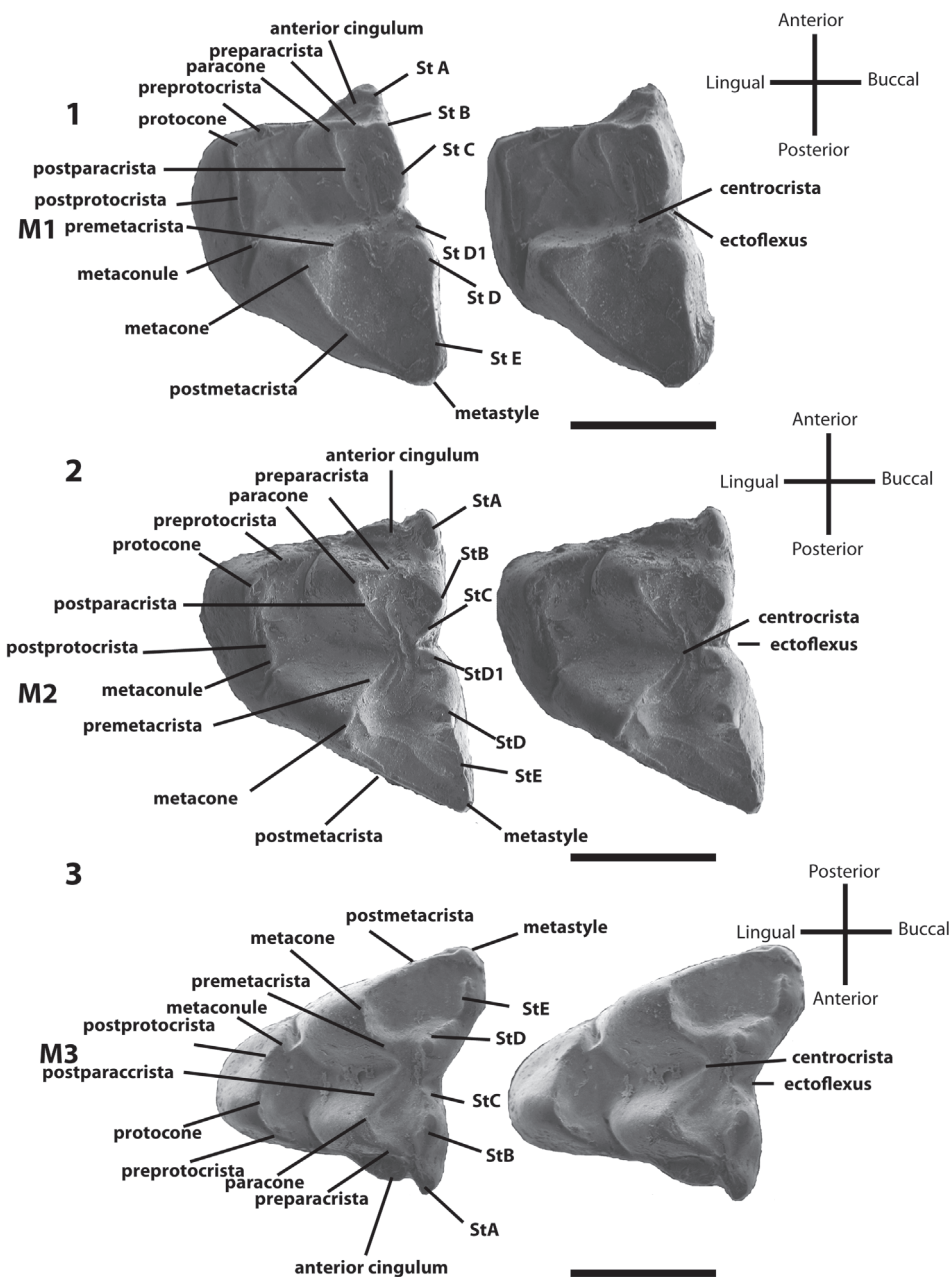


FIGURE 2. *Bulungu muirheadae*, sp. nov. Paratype UCR 15207, **1**, occlusal view stereo pair of M1. Paratype QM F10664, **2**, occlusal view stereo pair of M2. Paratype UCR 15275, **3**, occlusal view stereo pair of M3. Scale bar equals 1mm.

anterior cingulid extends from buccal flank of paraconid to anterobuccal flank of protoconid. Paraconid anterobuccally positioned relative to metaconid. Metaconid posterolingually positioned with respect to protoconid. Talonid wider than trigonid. Entoconid is oval in shape, with short preentocristid connecting it to posterior flank of metaconid. Small cingulid-like hypoconulid, posterobuccal to entoconid, connects to hypoconid via posthypocristid. Almost linear cristid obliqua

extends from hypoconid to posterobuccal flank of protoconid. Very small low ridge occurs posterobuccal to protoconid. Posterior cingulid absent.

Morphology of m2 similar to that of m1 except as follows. Paraconid more lingually positioned, almost directly anterior to metaconid. Protoconid more buccally-positioned increasing length of paracristid and metacristid. Distance between paraconid and metaconid relatively shorter. Anterior cingulid larger, extending further anterobuccally.

Talonid wider with hypoconid positioned further anterobuccally, resulting in a longer posthypocristid, but shorter cristid obliqua. Angle formed by posthypocristid and cristid obliqua at hypoconid smaller. Cristid obliqua terminates more lingually, directly posterior to apex of protoconid. Entoconid is wider, almost conical, with short postentocristid running perpendicular to preentocristid. Postentocristid increases in length with wear.

Morphology of m3 similar to that of m2 except as follows. Paraconid-metaconid distance shorter. Talonid shorter, with hypoconid positioned further anteriorly, decreasing length of cristid obliqua. Entoconid shorter in length, almost completely conical, despite retaining preentocristid.

Morphology of m4 similar to that of m3 except as follows. Distance between paraconid and metaconid greater, almost equal to paraconid-protoconid distance and metaconid-protoconid distance. Talonid reduced, with hypoconid positioned posterolingual to protoconid. Hypoconulid small. Cristid obliqua longer than in m3 and terminates against trigonid posterior flank, level with midpoint between protoconid and metaconid. Angle between cristid obliqua and posthypocristid relatively wider. Entoconid small but taller than hypoconid. Well-defined preentocristid extends anteriorly from entoconid and ends against posterior flank of metaconid. A short postentocristid extends from tip of entoconid posteriorly to position just anterior to hypoconulid.

Upper Dentition

The description of M1 is based on UCR 15307 (Figure 2). It is anteroposteriorly longer than buccolingually wide. StD tallest cusp on crown. Small cusp (StD1, sensu Turnbull et al., 2003) immediately anterior to StD. Large StC very slightly smaller than StD and positioned anterior to StD1, immediately anterior to ectoflexus. A crest connects StD1 to StC through the ectoflexus and connects anteriorly to StB. Paracone directly lingual to StB; preparacrista connects these two cusps. Postparacrista longer than preparacrista and connects to premetacrista just lingual to ectoflexus. Premetacrista longer than postparacrista, but shorter than postmetacrista. Metacone directly lingual to StD. Distance between these two cusps twice as long as distance between StB and paracone. Postmetacrista ends at most posterobuccal end of tooth and connects to stylar crest, which connects StD to metastyle via small remnant of StE. Anteriorly to StD, this crest does not connect to StD1 but instead, curves lingually. StA/para-

style just anterior to StB with small crest present running anteroposteriorly from most anterior part of tooth; this small crest ends prior to StB. Small anterior cingulum occurs lingual to StA, ending at a point just anterobuccal to paracone. Preprotocrista connects protocone to anterolingual base of paracone. Postprotocrista connects to small metaconule just lingual to base of metacone and ends posterolingual to latter. No posterior cingulum.

The description of M2 is based on QM F10664 (Figure 2). Morphology of M2 similar to that of M1 except as follows. Crown wider, with protocone more lingually situated. Metaconule smaller and more buccally situated. StA taller. Larger, more anteriorly and more lingually situated anterior cingulum. Paracone more posterolingually situated, increasing length of preparacrista and reducing length of postparacrista. StB much taller, almost as tall as StD and more posteriorly situated, increasing distance between it and StA. Connection between preparacrista and StB weaker, with anterior part of StB more rounded. StC highly reduced and as tall as StD1. StE reduced, almost indistinguishable along stylar crest between StD and metastyle.

The description of M3 is based on UCR 15275 (Figure 2). Morphology of M3 similar to that of M2 except as follows. Crown wider than long, with protocone more lingually situated. Anterior cingulum larger and more anteriorly extensive. Crest running through StA anteroposteriorly connects to anterior flank of StB. Preparacrista runs toward midpoint of StA's crest before curving anteriorly parallel to this crest, ending below StA. Angle between preparacrista and postparacrista wider. StC minute, barely visible above crest connecting StB to StD. StD1 absent. StE distinct, taller cusp. StE and metastyle more buccally situated, elongating postmetacrista. No stylar crest runs between StD and StE.

Measurements of upper and lower dentitions presented in Tables 1-2. Average body mass estimated to 135.58 grams.

BULUNGU CAMPBELLI, sp. nov.

Figure 3

<http://zoobank.org/15133E7C-0456-46F3-8DE0-A2CF72C6A006>

Specific Diagnosis

Bulungu campbelli differs from *B. palara* and *B. muirheadae* in the following combination of features: StA and StB connected by a crest on M3; StE absent on M3; postparacrista and premetacrista not connected to form a complete centrocrista

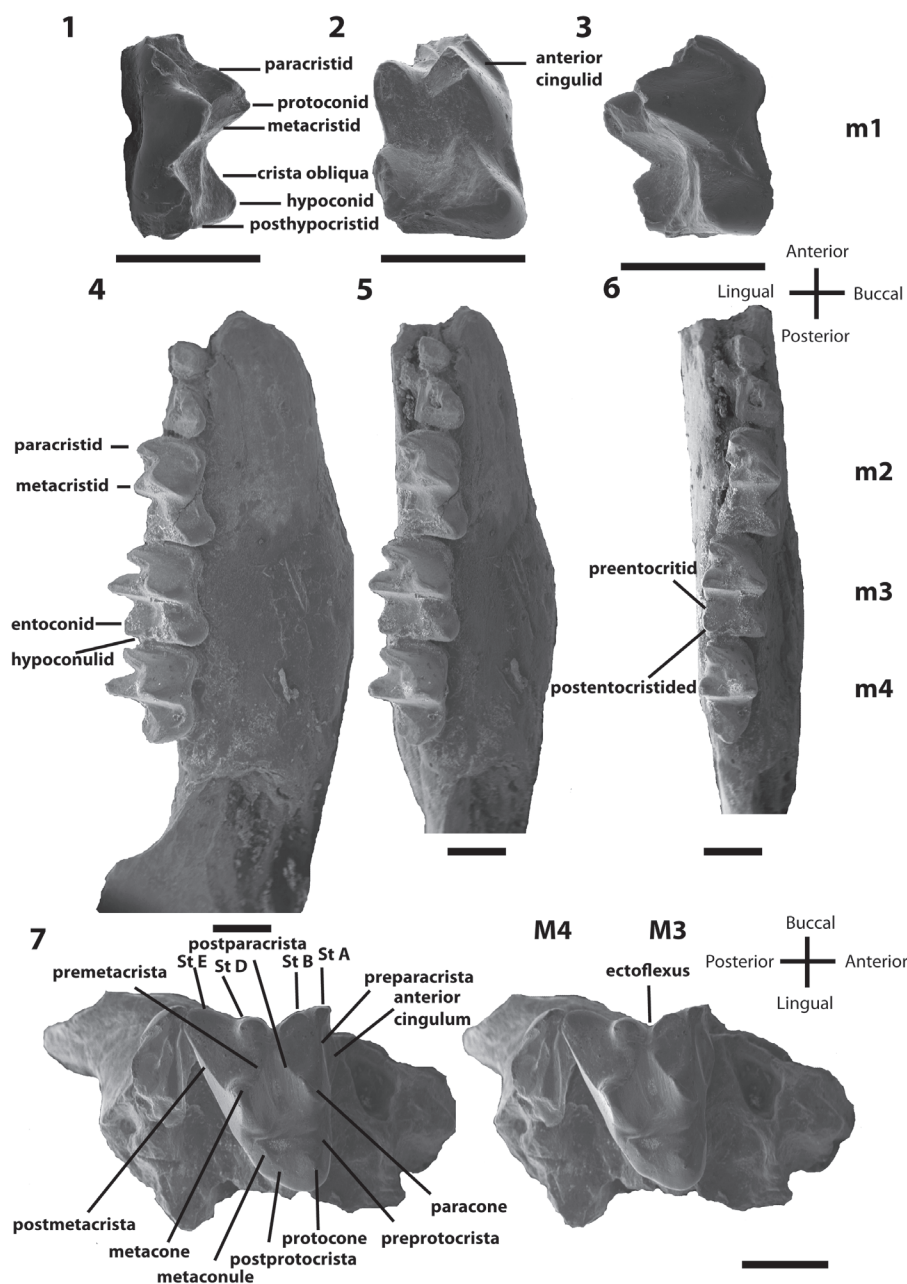


FIGURE 3. *Bulungu campbelli*, sp. nov. Holotype SAM P13853, **1**, lingual view of m1; **2**, occlusal view of m1; **3**, buccal view of m1; **4**, buccal view of right dentary; **5**, buccal/occlusal view of right dentary; **6**, occlusal view of right dentary; **7**, stereo pair of occlusal view of right maxilla. Scale bar equals 1mm.

on M3, but instead postparacrasta ends on lingual flank of StC, and premetacrasta ends on lingual flank of StD; metaconule on M3 minute and situated on lingual flank of metacone; metacristid perpendicular to tooth row on m3 only; postentocristid present; talonid slightly longer anteroposteriorly than trigonid on m3.

Specific Etymology

The species name honours vertebrate palaeontologist Colin Campbell for his significant contributions to peramelemorphian systematics and in particular the preliminary analysis in his PhD thesis (Campbell, 1976) of specimens referable to the taxa named and described here.

Holotype

SAM P13853, right dentary with m1-4 (Figure 3) and associated right maxilla fragment with M3 and partial M4 (Figure 3).

Type Locality

Ngapakaldi Quarry, site code V 5858, Lake Ngapakaldi, Etadunna Formation, Ngapakaldi LF, Zone C.

Age and Stratigraphy

The Ngapakaldi LF, (Etadunna Zone C) was regarded by Woodburne et al. (1993) to be late Oligocene in age, between 24-26 m.y.a. Based on palaeomagnetic and drill-core data, Metzger and Retallack (2010) estimated the Etadunna Formation to span from 26.1 to 23.6 m.y.a. The Ngapakaldi LF is therefore late Oligocene in age, but younger than the underlying Ditjimanka LF (Etadunna Zone B).

DESCRIPTION

Dentary

Dentary poorly preserved, missing anterior section from the anterior root of m1 (Figure 3). Posterior part of dentary also missing. Preserved base of coronoid process forms an angle of 120 degrees with the ramus. Dentary is deepest below m3.

Lower Dentition

Only molars preserved. The m1 (originally intact in the dentary but now loose) roots are preserved in the alveoli. Anterior root smaller and rounder than posterior root (Figure 3). All cusps except hypoconid damaged at tips. Protoconid tallest cusp followed (in decreasing order) by metaconid, entoconid, paraconid, hypoconid, and hypoconulid (Figure 3). Narrow anterior cingulid damaged on anterolingual side of tooth. Very little of paraconid preserved. In occlusal view, paraconid anterolingual to protoconid and anterobuccal to metaconid. Metaconid posterolingual to protoconid; hence, metacristid not perpendicular to tooth row. Hypoconid positioned posterobuccal to protoconid. Cristid obliqua departs obliquely from tip of hypoconid and terminates on posterior flank of protoconid. Hypoflexid present as a small shelf between buccal flank of protoconid and anterior flank of hypoconid. Steeply inclined posthypocristid connects hypoconid to hypoconulid. Very little of hypoconulid preserved but would have been directly posterior to entoconid. Entoconid directly

posterior to metaconid. Entoconid narrow, with pre-entocristid visible on undamaged anterior surface; preentocristid terminates within valley separating entoconid and metaconid. Talonid wider than trigonid. No posterior cingulid.

The morphology of m2 resembles that of m1 except as follows. Anterior cingulid of m2 extends from base of paraconid, perpendicular to tooth row, then curves posterobuccally toward base of protoconid (Figure 3). Trigonid narrow, with metaconid and paraconid closer to each other than either is to protoconid. Distance between paraconid and protoconid greater than distance between metaconid and protoconid. Entoconid highly worn or damaged. Cristid obliqua terminates below centre of metacristid.

The morphology of m3 resembles that of m2 except as follows (Figure 3). Paraconid and metaconid closer together, narrowing trigonid. Metacristid perpendicular to tooth row and parallel to posthypocristid. Metaconid tallest cusp, followed by entoconid, protoconid, paraconid, hypoconulid and hypoconid. Preentocristid connects entoconid to posterior base of metaconid. Entoconid wider posteriorly than anteriorly, almost teardrop-shaped. Short crest (postentocristid) runs at an angle buccally, almost perpendicular to tooth row, and ends near base of entoconid. Trigonid and talonid wider but shorter in length than on m2.

The morphology of m4 resembles that of m3 except as follows (Figure 3). Distances between paraconid and protoconid, and metaconid and protoconid all shorter. Angle formed by trigonid blades wider. Metaconid remains tallest cusp but followed by protoconid, paraconid, entoconid, hypoconid, and hypoconulid. Talonid reduced. Hypoconid more lingually situated, almost level with middle of metacristid. Very small hypoconulid posterobuccal to entoconid. These two cusps connected by postentocristid. Cristid obliqua runs anteriorly from the posterior flank of the trigonid, just buccal to the anterior tip of preentocristid and ends posteriorly at the tip of hypoconid, joining with posthypocristid at 120 degree angle. Posthypocristid ends at posterior extremity of tooth.

Upper Dentition

The maxilla (Figure 3) is poorly preserved. Only the alveoli for M2, the M3, and the anterior tip of M4 are preserved.

M3 is wider than long (Figure 3). Preparacrista extends from paracone in a buccal direction then curves anteriorly to join StA. A styler crest extends from tip of StA posteriorly, then curves lingually

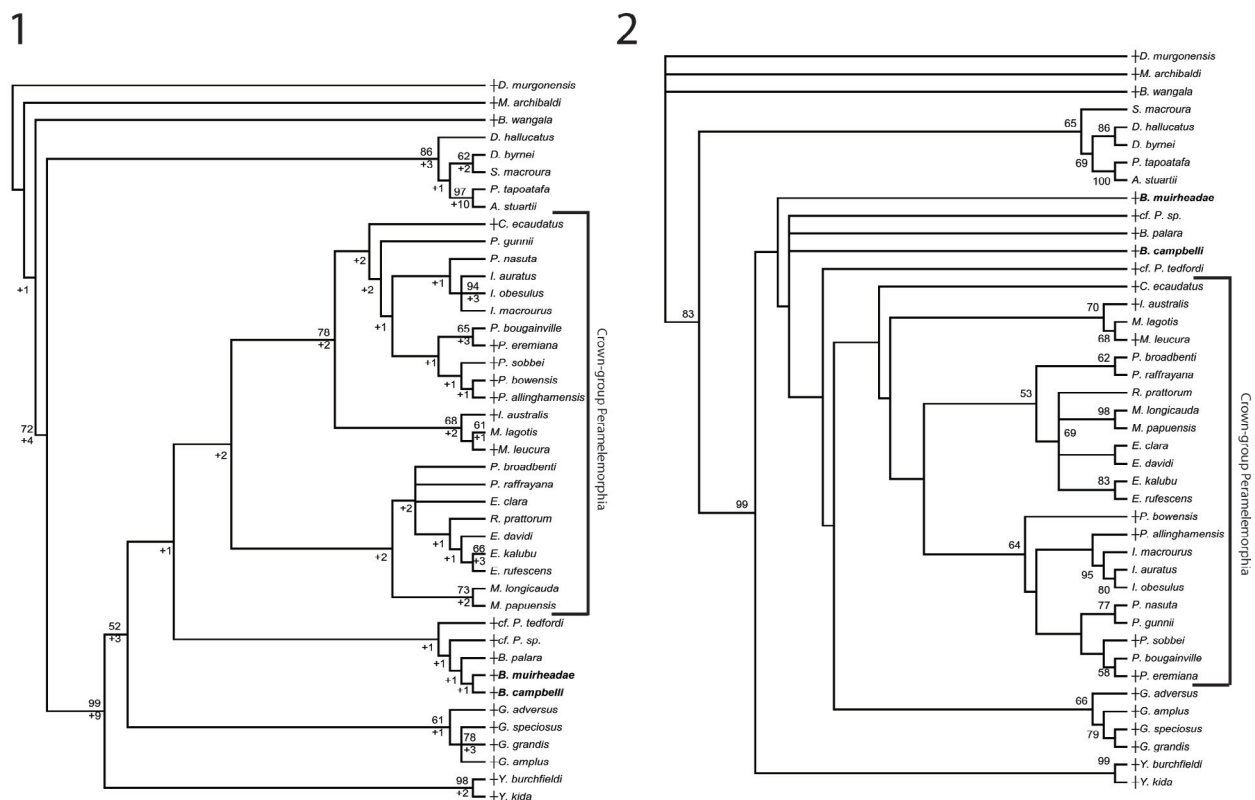


FIGURE 4. Phylogenetic relationships of *Bulungu muirheadae* and *B. campbelli* sp. nov. based on our 156 character craniodental matrix. Fossil and recently extinct taxa are indicated by †. *Bulungu muirheadae* and *B. campbelli* are highlighted in bold. Crown-group Peramelemorphia is bracketed. **1**, strict consensus of 8 most parsimonious trees (tree length = 889; consistency index excluding uninformative characters = 0.3412; retention index = 0.6560) from unconstrained maximum parsimony analysis of the matrix. Numbers above branches represent bootstrap values (1000 replicates); numbers below branches represent decay indices. **2**, strict consensus of 24 most parsimonious trees (tree length = 917; consistency index excluding uninformative characters = 0.3308; retention index 0.6395) that result when the matrix is analysed using maximum parsimony and enforcing a “backbone” molecular scaffold based on Westerman et al. (2012).

before curving again at the posterior flank of StA buccally to connect to tip of StB. This crest then continues posteriorly through a minute StC and ends prior to reaching the ectoflexus region. StD1 absent. No styler crest connects StD to metastyle. StE absent. Postparacrista straight, obliquely orientated and ends at base of posterolingual flank of StC. Postparacrista does not join premetacrista, and hence the centrocrista is incomplete. Premetacrista ends at anterolingual base of flank of StD. Postmetacrista longest crest and runs from metacone to metastyle. Anterior cingulum is wide and runs lingually from lingual flank below StA to almost level with middle of preparacrista. Protocone posterolingual to paracone. Preprotocrista runs parallel to preparacrista from anterior flank of paracone to protocone, and forms an angle of almost 90 degrees with postprotocrista. Postprotocrista then curves posteriorly almost parallel to

tooth row and joins small metaconule, before ending on lingual flank of metacone. Metaconule directly lingual to metacone. Posterior cingulum absent.

Very little of M4 is preserved (Figure 3). What can be seen resembles the anterior part of M3 but differs as follows. StA large and tall. Preparacrista runs from paracone to StA, parallel to preparacrista of M3. Styler crest runs obliquely from StA to the broken edge of the tooth. Morphology of anterior cingulum same as in M3.

Measurements of the upper dentition of *B. campbelli* are presented in Table 1 and of the lower dentition in Table 2. Average body mass estimated to 112.87 grams.

RESULTS

Unconstrained maximum parsimony analysis of our 156 craniodental character matrix recovered

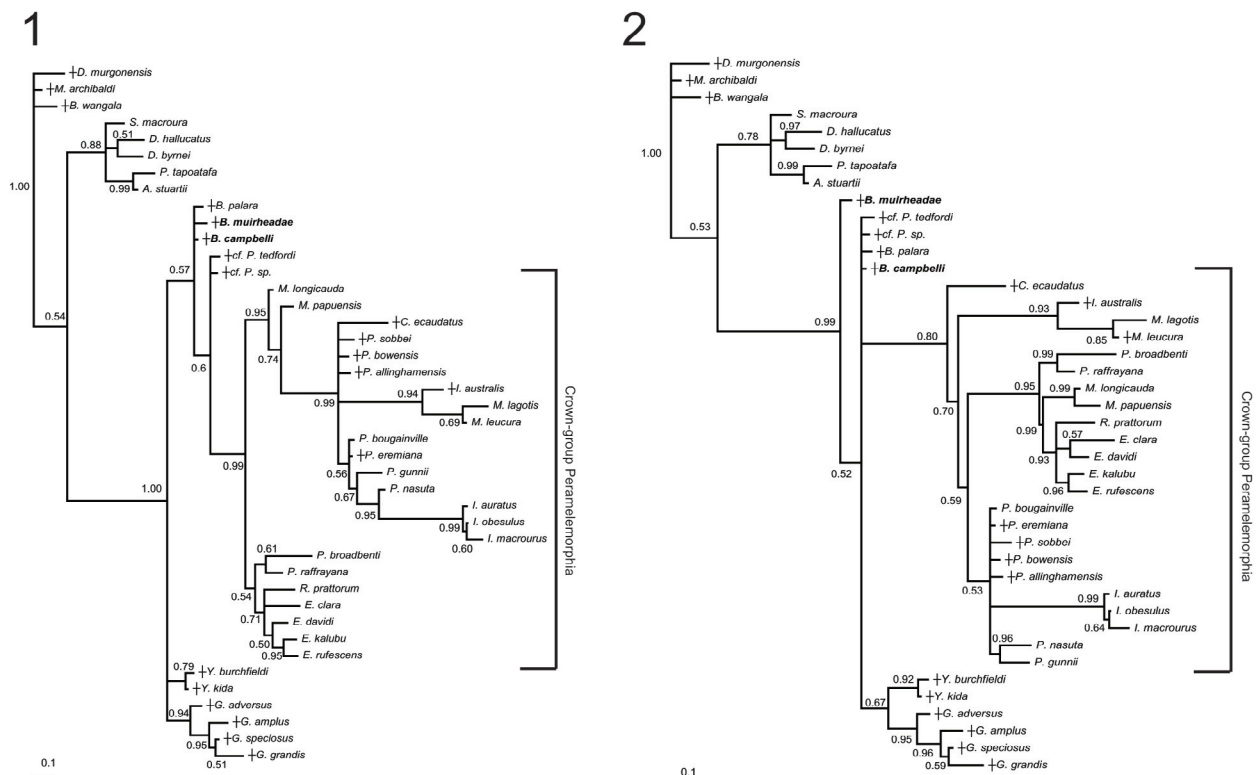


FIGURE 5. Phylogenetic relationships of *Bulungu muirheadae* and *B. campbelli* sp. nov. based on our 156 character craniodental matrix. Fossil and recently extinct taxa are indicated by †. *Bulungu muirheadae* and *B. campbelli* are highlighted in bold. Crown-group Peramelemorphia is bracketed. **1**, 50% majority rule consensus that results after Bayesian analysis of the matrix assuming the Mk + G model (harmonic mean of the log likelihood of the post-burn-in trees = -2898.10). The analysis was run for five million generations, sampling trees every 100 generations, with a “burn-in” period of 1.25 million generations. Numbers above branches represent Bayesian posterior probabilities. **2**, 50% majority rule consensus that results after Bayesian analysis of the matrix is analysed enforcing a “backbone” molecular scaffold based on Westerman et al. (2012), assuming the Mk + G model (harmonic mean of the log likelihood of the post-burn-in trees = -2933.45). The analysis was run for five million generations, sampling trees every 100 generations, with a “burn-in” period of 1.25 million generations. Numbers above branches represent Bayesian posterior probabilities.

8 most parsimonious trees of 889 steps; the strict consensus of these is illustrated in Figure 4.1, with bootstrap values above the branches and decay indices below. Parsimony analysis of the same matrix but enforcing a molecular scaffold as a “backbone” constraint recovered 24 most parsimonious trees of 917 steps, the strict consensus of which is given in Figure 4.2, with bootstrap values given above the branches. Unconstrained Bayesian analysis of the same matrix resulted in a post-burn-in log likelihood (harmonic mean) of -2898.10, whereas the post-burn-in log likelihood for the Bayesian analysis with the molecular scaffold enforced was -2933.45; the 50% majority rule consensus from the unconstrained and molecular scaffold Bayesian analyses are given in Figures

5.1 and 5.2, respectively, with Bayesian posterior probabilities given at the nodes.

In all four phylogenetic analyses presented here, *Bulungu campbelli* and *B. muirheadae* lie outside crown-group Peramelemorphia. Monophyly of *Bulungu* is recovered in the unconstrained maximum parsimony analysis, but with weak support (bootstrap <50%; decay index +1; Figure 4.1). However, the relationships of the three *Bulungu* species are unresolved in the unconstrained Bayesian analysis (Figure 5.1), and *B. palara* and *B. campbelli* are recovered as closer to the crown-group than is *B. muirheadae* in both parsimony and Bayesian analyses when a molecular scaffold is enforced (Figures 4.2, 5.2). The other Oligo-Miocene bandicoot taxa described to date, namely *Yarala burchfieldi*, *Y. kida* and the four species of

Galadi also lie outside crown-group Peramelemorphia in all four analyses, in agreement with the results of previous phylogenetic analyses (Travouillon et al., 2010; 2013; Gurovich et al., 2013). Monophyly of *Yarala* and *Galadi* is also relatively strongly supported in all four analyses. However, the relative branching order of *Bulungu*, *Yarala* and *Galadi* varies between the analyses, with *Bulungu* closer to the crown-group in the unconstrained parsimony and Bayesian analyses but more distant when a molecular scaffold was enforced.

Another notable feature of our analyses is the fact that the two bandicoot taxa described by Turnbull et al. (2003) from the early Pliocene Hamilton Fauna, namely cf. *Peroryctes tedfordi* and cf. *Peroryctes* sp., consistently fall outside the crown-group. In the unconstrained maximum parsimony analysis, these taxa form a clade with *Bulungu*, although this is not the case in the other three analyses. Based on these results, we believe that referral of these Pliocene taxa to *Peroryctes* is unjustified and that they are more likely late-surviving stem-peramelemorphians; if so, all known records of *Peroryctes* are from New Guinea, and crown-group peramelemorphians do not appear to be present in the Hamilton LF.

However, in contrast to the results of a previous study (Gurovich et al., 2013), analyses of our revised and expanded craniodental matrix consistently place the Pliocene *Ischnodon australis* in a clade with the Recent thylacomyids *Macrotis lagotis* and *M. leucura* with moderate-to-strong support, supporting the referral of *Ischnodon* to Thylacomyidae. The other Pliocene peramelemorphians, namely *Perameles allinghamensis* and *P. bowensis*, and the Pleistocene *P. sobbei* also consistently fall within the crown-group, and in all but the unconstrained Bayesian analysis form a clade with Recent *Perameles* and *Isodon* species (albeit with weak support); thus, our results confirm that *P. allinghamensis* and *P. bowensis* represent the oldest known records of the family Peramelidae (Peramelinae sensu Wilson and Reeder, 2005).

Our unconstrained maximum parsimony analysis shows greater congruence with current molecular phylogenies than do previous morphological analyses: monophyly of Peramelidae (i.e., *Perameles* + *Isodon*; = Peramelinae sensu Wilson and Reeder, 2005) to the exclusion of *Chaeropus* and thylacomyids, and of Peroryctidae (i.e., *Echymipera*+*Microperoryctes*+*Rhynchomeles*+*Peroryctes*) is supported, although *Chaeropus* and Thylacomyidae are placed as successive sister-

taxa to Peramelidae, rather than outside Peramelidae and Peroryctidae, as is the case in recent molecular phylogenies. By contrast, the unconstrained Bayesian analysis shows greater conflict: Peramelidae is not recovered as monophyletic to the exclusion of *Chaeropus* and thylacomyids, and Peroryctidae is recovered as paraphyletic. Nevertheless, the parsimony results are encouraging, and suggest that the increased taxon and character sampling in our craniodental matrix presented here has reduced the incongruence between morphological and molecular estimates of peramelemorphian phylogeny.

DISCUSSION

The origin of Peramelemorphia, like all marsupial orders in Australia, remains unclear. Recent phylogenetic analyses of higher-level marsupial relationships consistently place Peramelemorphia in a clade together with Dasyuromorphia and Notooryctemorphia (Beck, 2008, 2012; Beck et al., 2008b; Meredith et al., 2008, 2009, 2011; Nilsson et al., 2004), but the precise branching order between these three orders remains unclear. The oldest potential fossil record of Peramelemorphia may be as yet undescribed early Eocene specimens from the Tingamarra LF, near Murgon, southeastern Queensland (Black et al., 2012). Prior to the current paper, the oldest described bandicoot species were *Yarala kida* from the late Oligocene or early Miocene Kangaroo Well LF in the Northern Territory (Schwartz, 2006) and *Y. burchfieldi*, *Bulungu palara*, *Galadi speciosus*, *G. adversus*, *G. Amplus*, and *G. adversus* from early to late Miocene LFs of the Riversleigh WHA.

Fossil bandicoots from the late Oligocene Etadunna and early Miocene Wipajiri Formations of the Lake Eyre Basin, have been reported (Campbell, 1976; Woodburne et al., 1993; Case, 2001) but until now none has been formally described. Campbell (1976) reported two taxa: one small taxon from Zones B (Ditjimanka LF) and C (Ngapakaldi LF) and the Kutjamarpu LF (early Miocene), and one large taxon from the Kutjamarpu LF. The taxa described in this current paper and in Gurovich et al. (2013) are based on samples that include the specimens Campbell (1976) referred to the small species. With the advantage of additional specimens collected since Campbell's study, we have concluded that this material represents three distinct taxa: *Bulungu muirheadae* from the Ditjimanka LF (this work), *B. campbelli* from the Ngapakaldi LF (this work), and *B. palara* from the Kutjamarpu and several Riversleigh LFs

(Gurovich et al., 2013). Campbell's (1976) large species remains undescribed. It appears to be unique to the Kutjamarpu LF. However, we have identified a third species from the Kutjamarpu LF that is also known from Riversleigh Faunal Zone B (early Miocene) and C (mid Miocene) LFs. Woodburne et al. (1993) and Case (2001) note but do not name other peramelemorphian specimens from the Etadunna and Wipajiri Formations. Pending formal description of these specimens, their relationships to taxa described in this work remain uncertain.

The dental morphology (tribosphenic dentition, lacking development of the metaconule) and size of *Bulungu campbelli* (~112.87 grams, this work) and *B. muirheadae* (~135.58 grams, this work) is similar to that of *B. palara* (~130 grams, Gurovich et al., 2013) suggesting that they were small insectivores. Gurovich et al., 2013 noted that *B. palara*, along with *Yarala burchfieldi* (~75 grams, Travouillon et al., 2009) and *Y. kida* (Schwartz et al., 2006) were smaller than any living species of bandicoot. *B. muirheadae* and *B. campbelli* add to the diversity of small bodied bandicoots, which provide further support that Oligo-Miocene Australian peramelemorphians filled ecological niches that today are mostly occupied by dasyurids (Muirhead, 1994, 2000; Muirhead and Filan, 1995; Schwartz, 2006; Travouillon et al., 2010, 2013; Gurovich et al., 2013).

Bulungu muirheadae appears to be more plesiomorphic than either *B. campbelli* or *B. palara* in its retention of complete centrocristae on all upper molars. This is supported by two of our four phylogenetic analyses, where *Bulungu muirheadae* branches of earlier than the other two *Bulungu* species (Figures 4-5). Based on their craniodental morphology all of the Oligo-Miocene fossil peramelemorphians described to date, including *Bulungu campbelli* and *B. muirheadae* from the Etadunna formation described here, appear more plesiomorphic than any extant bandicoot (Muirhead and Filan, 1995; Muirhead, 2000; Travouillon et al., 2010, 2013; Gurovich et al., 2013). Previous studies (Travouillon et al., 2010, 2013; Gurovich et al., 2013), as well as the results of the more comprehensive phylogenetic analyses presented here (Figures 4-5), also suggest that all of these taxa lie outside crown-group Peramelemorphia. Our results indicate that the oldest described crown-group bandicoots are early Pliocene in age, namely the thylacomyid *Ischnodon australis* and the peramelids *Perameles allinghamensis* and *P. bowensis*.

These results appear to be in conflict with dated molecular phylogenies, which suggest that the earliest divergences among crown-group peramelemorphians occurred >20 m.y.a. (Meredith et al., 2008) or even 27 m.y.a. or older, depending on the method and calibrations used (Meredith et al., 2008, 2011; Westerman et al., 2012). These relatively ancient estimated divergence dates are possible, given the relatively scanty nature of the peramelemorphian fossil record and despite recent improvements in our knowledge. Nevertheless, if the South Australian, Northern Territory and Queensland Oligocene and Miocene fossil assemblages described to date are truly representative of peramelemorphian diversity at that time, this would imply that crown-group peramelemorphians were either much rarer than their stem-relatives or were restricted to geographical areas that have yet to be sampled, such as Western Australia. However, it should be noted that additional fossil species from Riversleigh (Archer et al., 2006) and the Lake Eyre Basin (Case, 2001) remain to be described, and could potentially include crown-group taxa.

Alternatively, it is possible that the molecular divergence dates are overestimates (see Gurovich et al., 2013). The latter possibility is perhaps rendered more likely by the fact that both Meredith et al. (2008) and Westerman et al. (2012) used "cf. *Peroryctes*" *tedfordi* and "cf. *Peroryctes*" sp. from the early Pliocene Hamilton fauna (Turnbull et al., 2003) to calibrate the split between *Peroryctes* (= Peroryctinae) and *Echymipera*+*Microperoryctes* (= Echymiperinae), whereas our phylogenetic analyses consistently place "cf. *Peroryctes*" *tedfordi* and "cf. *Peroryctes*" sp. outside crown-group Peramelemorphia, and hence neither fossil taxon is suitable for calibrating divergences within the crown-group (see below). As we note above, according to the results of our phylogenetic analyses, the oldest known crown-group peramelemorphians are the early Pliocene *Ischnodon australis* and the early Pliocene peramelids *Perameles allinghamensis* and *P. bowensis*, which, we argue, are suitable for specifying minimum dates for the Thylacomyidae-(Peramelidae+Peroryctidae) and Peramelidae-Peroryctidae splits, respectively. Although beyond the scope of the current paper, it would be interesting to see what impact the use of these alternative calibrations has on molecular divergence dates.

Given the occurrence of crown-group peramelemorphian clades in the Pliocene, namely Thylacomyidae (represented by *Ischnodon australis*) and Peramelidae (represented by *Perameles all-*

inghamensis and *P. bowensis*), it seems that these more modern groups had begun to supplant the archaic stem-lineages by this time, probably following a rapid but poorly documented interval of diversification in the late Miocene. Nevertheless, some stem-peramelemorphians appear to have survived this apparent late Miocene faunal turnover event, as indicated by the presence of “cf. *Peroryctes tedfordi*” and “cf. *Peroryctes*” sp. (both of which were consistently recovered outside the crown-group in our phylogenetic analyses) in the early Pliocene Hamilton LF. Interestingly, Hocknull (2005) described two peramelemorphian species from middle Pleistocene (Hocknull et al., 2007) cave deposits at Mount Etna, central-eastern Queensland that could not be referred to any modern family. Hocknull (2005) noted similarities between these species and both “cf. *Peroryctes tedfordi*” and *Yarala burchfieldi*. It is therefore possible that stem-peramelemorphians survived in Australia until at least the middle Pleistocene, perhaps going extinct with the onset of more xeric conditions some time after 280,000 years ago (Hocknull et al., 2007). It is worth mentioning that both Hamilton LF and the middle Pleistocene cave deposits at Mount Etna have been interpreted as rainforest environments. This could potentially suggest that stem-peramelemorphians were adapted to rainforest environments and that they survived in these relictual habitats.

If the early Pliocene “cf. *Peroryctes tedfordi*” and “cf. *Peroryctes*” sp. and the two middle Pleistocene peramelemorphian species described by Hocknull (2005: 78) belong to stem-Peramelemorphia rather than to the extant family Peroryctidae, then peroryctids are currently unknown from Australia, with the sole exception of the extant *Echymipera rufescens*, which appears to have dispersed to Australia from New Guinea during the Plio-Pleistocene. Thus, it is possible that the early evolutionary of peroryctids was restricted to New Guinea (contra Westerman et al., 2012). However, this hypothesis must be weighed against geological evidence (Quarles van Ufford and Cloos, 2005, summarised by Westerman et al., 2012) that suggests that only small areas of land were emergent off the north coast of the Australian continent prior to ~12 m.y.a., and that these were separated from Australia by deepwater barriers. In this context, accurate estimates of divergence times within Peramelemorphia and other marsupial clades (e.g., Pseudocheiridae, Meredith et al., 2009; Phalangeridae, Raterman et al., 2006) will be key to under-

standing the differential roles that the Australian mainland and New Guinea played in the diversification of marsupials in the Australo-Papuan region. Given the essential role that fossils play in calibrating molecular divergence dates, a better understanding of the fossil record and phylogeny of Peramelemorphia will be crucial to this endeavour, as will improvements in molecular sampling and methods (dos Reis et al., 2012).

In terms of overall peramelemorphian diversity through time, although inferences based on raw taxon counts (which do not take into account geological, taphonomic, collecting or other biases) should be treated as highly tentative, taxonomic diversity appears to have been relatively low during the late Oligocene, with no more than two species known from any one site (Case, 2001). In the early Miocene, diversity seems to have significantly increased, with some Riversleigh fossil localities containing seven different species (Archer et al., 2006). In the middle Miocene, a maximum of five species have been recorded at Gag Site at Riversleigh. In the late Miocene, two species have been reported from Encore Site in Riversleigh (Myers et al., 2001) and two specimens (unclear whether these specimens represent 1 or 2 species) from Alcoota (Murray and Megirian, 1992). Whether the apparent drop in peramelemorphian diversity seen in the late Miocene is related to the inferred faunal turnover event discussed above will require more detailed study of appropriately aged sites; unfortunately, the late Miocene vertebrate fossil record is poorly known in Australia, particularly for small mammals (Archer et al., 1999).

CONCLUSIONS

Two small, insectivorous peramelemorphian marsupials, *Bulungu muirheadae* and *B. campbelli*, are described from the late Oligocene of the Etadunna Formation, one from the Ditjimanka LF and one from the Ngapakaldi LF in central Australia. These two are related to a third species, *Bulungu palara*, from the Miocene Kutjamarpu LF of central Australia and several LFs from Riversleigh in northwestern Queensland. The two new species are currently among the oldest formally described bandicoots. The results of our phylogenetic analysis also reveal that early Pliocene “cf. *Peroryctes tedfordi*” and “cf. *Peroryctes*” sp. from Hamilton LF belong to stem-Peramelemorphia rather than to the extant family Peroryctidae.

ACKNOWLEDGMENTS

Support for research at Riversleigh has come from the Australian Research Council (DP0453262, LP0453664, LP0989969 and LP100200486 grants to M. Archer and S.J. Hand and DE120100957 to R.M.D. Beck at the University of New South Wales); XSTRATA Community Partnership Program (North Queensland); the University of New South Wales; Phil Creaser and the CREATE Fund, the Queensland National Parks and Wildlife Service; Environment Australia; the Queensland Museum; the Riversleigh Society Inc.; Outback at Isa; Mount Isa City Council; and private supporters including K. and M. Pettit, E. Clark, M. Beavis and M. Dickson. Assistance in the field has come from many hundreds of volunteers as well as staff and postgraduate students of the University of New South Wales. Assistance in central Australia came from the University of California, Berkeley with significant input in the field from C. Campbell, M. Woodburne and B. Clemens. We thank C. Campbell for enabling us to study the bandicoots he examined during his PhD research. We thank R. Day for providing funding to the University of Queensland to create a postdoctoral position for K.J. Travouillon. We thank S. Ingleby and A. Divljan from the Australian Museum, H. Janetzki from the Queensland Museum and C. Stevenson from the Western Australian Museum for providing access to the modern bandicoot collections. We thank the UNSW Palaeosciences Lab and the UQ Palaeo Hub for their support and anonymous reviewers for helpful comments.

REFERENCES

- Aplin, K.P. and Archer, M. 1987. Recent advances in marsupial systematics with a new syncretic classification, p. xv-lxxii. In Archer, M. (ed.), *Possums and Opossums, Studies in Evolution*. Surrey Beatty and Sons, Sydney, Australia.
- Archer, M. 1976. The dasyurid dentition and its relationships to that of didelphids, thylacinids and borhyaenids. *Australian Journal of Zoology*, Supplementary Series 39:1-34.
- Archer, M. and Wade, M. 1976. Results of the Ray E. Lemley expeditions, part 1: The Allingham Formation and a new Pliocene vertebrate fauna from northern Queensland. *Memoirs of the Queensland Museum*, 17:54-58.
- Archer, M., Arena, D.A., Bassarova, M., Beck, R.M.D., Black, K., Boles, W.E., Brewer, P., Cooke, B.N., Crosby, K., Gillespie, A., Godthelp, H., Hand, S.J., Kear, B.P., Louys, J., Morrell, A., Muirhead, J., Roberts, K.K., Scanlon, J.D., Travouillon, K.J., and Wroe, S. 2006. Current status of species-level representation in faunas from selected fossil localities in the Riversleigh World Heritage Area, northwestern Queensland. *Alcheringa Special Issue*, 1: 1-17.
- Archer, M., Arena, R., Bassarova, M., Black, K., Brammall, J., Cooke, B., Creaser, P., Crosby, K., Gillespie, A., Godthelp, G., Gott, M., Hand, S.J., Kear, B., Krikmann, A., Mackness, B., Muirhead, J., Musser, A., Myers, T., Pledge, N., Wang, Y., and Wroe, S. 1999. The evolutionary history and diversity of Australian mammals. *Australian Mammalogy*, 21:1-45.
- Beck, R.M.D. 2008. A dated phylogeny of marsupials using a molecular supermatrix and multiple fossil constraints. *Journal of Mammalogy*, 89:175-189.
- Beck, R.M.D. 2012. An 'ameridelphian' marsupial from the early Eocene of Australia supports a complex model of Southern Hemisphere marsupial biogeography. *Naturwissenschaften*, 99:715-29.
- Beck, R.M.D., Godthelp, H., Weisbecker, V., Archer, M., and Hand, S.J. 2008b. Australia's oldest marsupial fossil and their biogeographical implications. *PLoS ONE*, 3:e1858.
- Beck, R.M.D., Archer, M., Godthelp, H., Mackness, B.S., Hand, S.J., and Muirhead, J. 2008a. A bizarre new family of Marsupialia (Incertae sedis) from the early Pliocene of northeastern Australia: implications for the phylogeny of bunodont marsupials. *Journal of Paleontology*, 82:749-762.
- Black, K.H., Archer, M., Hand, S.J., and Godthelp, H. 2012. The rise of Australian marsupials: a synopsis of biostratigraphic, phylogenetic, palaeoecologic and palaeobiogeographic understanding. In Talent, J.A., (ed.), *Earth and Life: Global Biodiversity, Extinction Intervals and Biogeographic Perturbations Through Time*. Dordrecht: Springer. pp. 983-1078.
- Campbell, C.R. 1976. *Tertiary Dasyuridae and Peramelidae (Marsupialia) from the Tirari Desert, South Australia*. Unpublished PhD Thesis, University of California, Berkeley, USA.
- Case, J. A. 2001. Turnover of bandicoots in the Oligo-Miocene of South Australia. *Journal of Vertebrate Paleontology*, 21:39A.
- dos Reis, M., Inoue, J., Hasegawa, M., Asher, R.J., Donoghue, P.C.J., and Yang, Z. 2012. Phylogenomic datasets provide both precision and accuracy in estimating the timescale of placental mammal phylogeny. *Proceedings of the Royal Society B*, 279:3491-3500.
- Eriksson, T. 2001. AutoDecay ver. 5.0. Bergius Foundation, Royal Swedish Academy of Sciences, Stockholm.
- Gurovich, Y., Travouillon, K.J., Beck, R.M.D., Muirhead, J., and Archer, M. 2013. Biogeographical implications of a new mouse-sized fossil bandicoot (Marsupialia: Peramelemorphia) occupying a dasyurid-like ecological niche across Australia. *Journal of Systematic Paleontology*, DOI:10.1080/14772019.2013.776646.

- Hocknull, S.A. 2005. Ecological succession during the late Cainozoic of central eastern Queensland: extinction of a diverse rainforest community. *Memoirs of the Queensland Museum*, 51:39-122.
- Hocknull, S.A., Zhao, J.-x., Feng, Y.-x., and Webb, G.E. 2007. Responses of Quaternary rainforest vertebrates to climate change in Australia. *Earth and Planetary Science Letters*, 264: 317-331.
- Kirsch, J.A.W. 1968. Prodomus of the comparative serology of Marsupialia. *Nature*, 217:418-420.
- Krajewski, C., Torunsky, R., Sipiowski, J.T., and Westerman, M. 2007. Phylogenetic relationships of the dasyurid marsupial genus *Murexia*. *Journal of Mammalogy*, 88:696-705.
- Lewis, P.O. 2001. A likelihood approach to inferring phylogeny from discrete morphological characters. *Systematic Biology*, 50:913-925.
- Luckett, W.P. 1993. An ontogenetic assessment of dental homologies in therian mammals, p. 182-204. In Szalay, F.S., Novacek, M.J., and McKenna, M.C. (eds.), *Mammal Phylogeny: Mesozoic Differentiation, Multituberculates, Monotremes, Early Eutherians and Marsupials*. Springer-Verlag, New York.
- Meredith, R.W., Westerman, M., and Springer, M.S. 2008. A timescale and phylogeny for "Bandicoots" (Peramelemorphia: Marsupialia) based on sequences for five nuclear genes. *Molecular Phylogenetics and Evolution*, 47:1-20.
- Meredith, R.W., Krajewski, C., Westerman, M., and Springer, M.S. 2009. Relationships and divergence times among the orders and families of Marsupialia. *Museum of Northern Arizona Bulletin*, 65:383-406.
- Meredith, R.W., Janecka, J.E., Gatesy, J., Ryder, O.A., Fisher, C.A., Teeling, E.C., Goodbla, A., Eizirik, E., Simao, T.L.L., Stadler, T., Rabosky, D.L., Honeycutt, R.L., Flynn, J.J., Ingram, C.M., Steiner, C., Williams, T.L., Robinson, T.J., Burk-Herrick, A., Westerman, M., Ayoub, N.A., Springer, M.S., and Murphy, W.J. 2011. Impacts of the Cretaceous terrestrial revolution and KPg extinction on mammal diversification. *Science*, 334:521-524.
- Metzger, C.A. and Retallack, G.J. 2010. Paleosol record of Neogene climate change in the Australian outback. *Australian Journal of Earth Sciences*, 57:871-885.
- Muirhead, J. 1994. *Systematics, evolution and palaeobiology of recent and fossil bandicoots (Peramelemorphia, Marsupialia)*. Unpublished PhD Thesis, University of New South Wales, Sydney, Australia.
- Muirhead, J. 2000. Yaraloidea (Marsupialia, Peramelemorphia), a new superfamily of marsupial and a description and analysis of the cranium of the Miocene *Yarala burchfieldi*. *Journal of Paleontology*, 74:512-523.
- Muirhead, J. and Filan, S.L. 1995. *Yarala burchfieldi*, a plesiomorphic bandicoot (Marsupialia, Peramelemorphia) from Oligo-Miocene deposits of Riversleigh, northwestern Queensland. *Journal of Paleontology*, 69:127-134.
- Muirhead, J., Dawson, L., and Archer, M. 1997. *Perameles bowensis*, a new species of *Perameles* (Peramelemorphia, Marsupialia) from Pliocene faunas of Bow and Wellington caves, New South Wales. *Proceedings of the Linnean Society of New South Wales*, 17:163-174.
- Murray, P. and Megirian, D. 1992. Continuity and contrast in middle and late Miocene vertebrate communities from Northern Territory, p. 195-218. In Murray, P.F. and Megirian, D. (eds.), *Proceedings of the 1991 Conference on Australasian Vertebrate Evolution, Palaeontology and Systematics, The Beagle, Records of the Northern Territory Museum of Arts and Sciences*, Alice Springs, Australia.
- Myers, T.J. 2001. Prediction of marsupial body mass. *Australian Journal of Zoology*, 49:99-118.
- Myers, T.J., Crosby, K., Archer, M., and Tyler, M. 2001. The Encore local Fauna, a late Miocene assemblage from Riversleigh, northwestern Queensland. *Memoirs of the Association of Australasian Palaeontologists*, 25:147-154.
- Nilsson, M.A., Arnason, U., Spencer, P.B.S., and Janke, A. 2004. Marsupial relationships and a timeline for marsupial radiation in South Gondwana. *Gene*, 340:189-196.
- Price, G.J. 2002. *Perameles sobbei*, sp. nov. (Marsupialia, Peramelidae), a Pleistocene bandicoot from the Darling Downs, south-eastern Queensland. *Memoirs of the Queensland Museum*, 48:193-197.
- Price, G. J. 2005. Fossil bandicoots (Marsupialia, Peramelidae) and environmental change during the Pleistocene on the Darling Downs, southeastern Queensland, Australia. *Journal of Systematic Palaeontology*, 4:347-356.
- Quarles van Ufford, A. and Cloos, M. 2005. Cenozoic tectonics of New Guinea. *American Association of Petroleum Geologists Bulletin*, 89:119-140.
- Raterman, D., Meredith, R.W., Reudas, L.A., and Springer, M.S. 2006. Phylogenetic relationships of the cuscuses and brushtail possums (Marsupialia: Phalangeridae) using the nuclear gene BRCA1. *Australian Journal of Zoology*, 54:353-361.
- Schwartz, L.R.S. 2006. A new species of bandicoot from the Oligocene of Northern Australia and implications of bandicoots for correlating Australian Tertiary mammal faunas. *Palaeontology*, 49:991-998.
- Stirton, R.A. 1955. Late Tertiary marsupials from South Australia. *Records of the South Australian Museum*, 11:247-268.
- Swofford, D. L. 2002. PAUP*. Phylogenetic Analysis Using Parsimony (*and Other Methods). Version 4 (updated to 10 beta). Sinauer Associates, Sunderland, Massachusetts.

- Travouillon, K.J., Gurovich, Y., Beck, R.M.D., and Muirhead, J. 2010. An exceptionally well-preserved short-snouted bandicoot (Marsupialia; Peramelemorphia) from Riversleigh's Oligo-Miocene deposits, north-western Queensland, Australia. *Journal of Vertebrate Paleontology*, 30:1528-1546.
- Travouillon, K.J., Legendre, L., Archer, M., and Hand, S. 2009. Palaeoecological analyses of Riversleigh's Oligo-Miocene sites: Implications for Oligo-Miocene climate change in Australia. *Palaeogeography, Palaeoclimatology, Palaeoecology*, 276:24-37.
- Travouillon, K.J., Gurovich, Y., Archer, M., Hand, S.J., and Muirhead, J., 2013. The genus *Galadi*: three new bandicoots (Marsupialia; Peramelemorphia) from Riversleigh's Miocene deposits, north-western Queensland, Australia. *Journal of Vertebrate Paleontology*, 33:153-168.
- Turnbull, W.D., Lundelius, E.L.Jr., and Archer, M. 2003. Dasyurids, perameloids, phalangeroids, and vombatoids from the early Pliocene Hamilton fauna, Victoria, Australia. *Bulletin of the American Museum of Natural History*, 279:513-540.
- Westerman, M., Young, J., and Krajewski, C. 2008. Molecular relationships of *Pseudantechinus*, *Parantechinus*, and *Dasykaluta* (Marsupialia: Dasyuridae). *Australian Mammalogy*, 29:201-212.
- Westerman, M., Kear, B.P., Aplin, K., Meredith, R.W., Emerling, C., and Springer, M.S. 2012. Phylogenetic relationships of living and recently extinct bandicoots based on nuclear and mitochondrial DNA sequences. *Molecular Phylogenetics and Evolution*, 62:97-108.
- Wilson, D.E. and Reeder D.M. 2005. *Mammal Species of the World. A Taxonomic and Geographic Reference* (third edition), Johns Hopkins University Press, Baltimore, USA.
- Woodburne, M.O. and Case, J.A. 1996. Dispersal, vicariance, and the late Cretaceous to early Tertiary land mammal biogeography from South America to Australia. *Journal of Mammalian Evolution*, 3:121-162.
- Woodburne, M.O., Macfadden, B.J., Case, J.A., Springer, M.S., Pledge, N., Power, J.D., Woodburne, J., and Springer, K.B. 1993. Land mammal biostratigraphy and magnetostratigraphy of the Etadunna Formation (late Oligocene) of South Australia. *Journal of Vertebrate Paleontology*, 13:483-515.
- Worthy, T.H., Tennyson, A.J.D., Archer, M., Musser, A.M., and Hand, S.J. 2006. Miocene mammal reveals a Mesozoic ghost lineage on insular New Zealand, southwest Pacific. *Proceedings of the National Academy of Sciences of the United States of America*, 103:19419-19423.

APPENDIX 1

List and description of 156 characters and states used in our phylogenetic analyses. Ordered characters are indicated with an asterisk (*).

1. Upper incisor number
 - (0) five incisors present
 - (1) four incisors present (I5 lost)
2. Diastema between I4 and I5
 - (0) absent
 - (1) present
3. I5 morphology
 - (0) I5 similar in morphology to I1-4
 - (1) I5 pointed and strongly canine-like
 - (2) I5 premolar like,
4. *Degree of development of lingual shelf on P3
 - (0) no shelf
 - (1) small/weakly developed shelf
 - (2) well-developed lingual shelf
 - (3) well-developed lingual shelf that extends to the buccal side of P3,
5. *P3 major cusp development
 - (0) P3 major cusp laterally compressed
 - (1) P3 major cusp laterally enlarged but not conical
 - (2) P3 major cusp large and conical, but P3 is narrower than M1
 - (3) P3 Major cusp large and conical, and P3 is wider than M1,
6. *Stylar crest on M1
 - (0) stylar crest present on StD connects to metastylar tip
 - (1) StD is a conical cusp not connected to the stylar crest running to the metastylar tip
 - (2) StD is a conical cusp and no stylar crest present,
7. *Anterior cingulum of M1
 - (0) no anterior cingulum
 - (1) small anterior cingulum lingual to anterior tip of tooth, no connection to talon
 - (2) anterior cingulum enlarged and connects to talon as small shelf,
8. *Anterior cingulum of M3
 - (0) no anterior cingulum
 - (1) small anterior cingulum lingual to anterior tip of tooth
 - (2) small anterior cingulum connected to protocone shelf by a small shelf
 - (3) large anterior cingulum expanded further up to the protocone,
9. *Direction of preparacrista of M1
 - (0) preparacrista anterobuccally orientated to connect to anteriorly positioned StB.
 - (1) preparacrista buccally orientated (perpendicular to tooth row) then posterobuccally orientated
 - (2) preparacrista posterobuccally orientated to connect to posteriorly located StB
 - (3) preparacrista posterobuccally orientated to connect to StB and then reconnects with postparacrista posteriorly,
10. *Posterior cingulum of M3
 - (0) absent
 - (1) present
 - (2) present and wide,
11. *Morphology of the centrocrista on M1 and M2
 - (0) postparacrista and premetacrista contact each other, forming a complete centrocrista that connects the paracone and metacone (more lingually).
 - (1) postparacrista and premetacrista contact each other, forming a complete centrocrista that connects the paracone and metacone (more buccally)
 - (2) postparacrista does not connect to the premetacrista and ends at the base of StB, premetacrista ends at base of StD ,
12. *Morphology of centrocrista on M3
 - (0) postparacrista and premetacrista contact each other, forming a complete centrocrista that connects the paracone and metacone (more lingually).
 - (1) postparacrista and premetacrista contact each other, forming a complete centrocrista that connects the paracone and metacone (more buccally)

- (2) postparacrista does not connect to the premetacrista and ends at the base of StB, premetacrista ends at base of StD ,
13. *Lobation of i3
 - (0) i3 is unicuspid
 - (1) i3 posterior cusp present but small
 - (2) I3 posterior cusp present and large,
 14. Length of p3
 - (0) p3 longer or equal in length to p2
 - (1) p3 shorter than p2 ,
 15. Presence of preentocristid
 - (0) present
 - (1) absent,
 16. Direction of preentocristid of m1-3
 - (0) anteroposterior
 - (1) oblique,
 17. Cusp within the hypoflexid region, between the talonid and trigonid on the buccal side
 - (0) no median buccal cusp present
 - (1) median buccal cusp present ,
 18. Distinction between lower molar crowns and roots
 - (0) crown distinct from roots
 - (1) crown and root indistinct (other than for limit of enamel)
 19. Hypoconulid posterior to entoconid
 - (0) hypoconulid positioned posterobuccal to the entoconid
 - (1) hypoconulid positioned almost directly posterior to the entoconid ,
 20. *Size of talonid on m4
 - (0) entoconid and hypoconid large, talonid relatively wide, crests clearly identifiable.
 - (1) entoconid and hypoconid smaller than in state 0, talonid smaller
 - (2) further reduction of entoconid and hypoconid, talonid very small, crest poorly defined,
 21. Snout length and premaxilla size
 - (0) premaxilla taller than it is long; maxilla-nasal contact longer than premaxilla-nasal contact (usually correlated with a relatively short snout)
 - (1) premaxilla longer than it is tall; premaxilla-nasal contact longer than maxilla-nasal contact (usually correlated with a relatively elongate snout) ,
 22. Width of nasals
 - (0) broad nasals
 - (1) slender nasals, not markedly expanded posteriorly ,
 23. *Position of nasal-frontal suture/maximum posterior extension of nasals
 - (0) posterior to the anterior rim of the orbit when viewed laterally
 - (1) nasals terminate just anterior to the orbit when viewed laterally (associated with a wide maxilla-frontal suture)
 - (0) nasals terminate well anterior to the anterior margin of the orbit,
 24. Infraorbital canal length
 - (0) long infraorbital canal (longer than half the molar row).
 - (1) short infraorbital canal (shorter or equal to half the molar row),.
 25. Jugal-maxilla contact
 - (0) jugal invades the maxilla and extends onto the facial region of the skull (not bifid)
 - (1) maxilla invades the zygomatic arch so that the jugal has two thin wings around the posterior maxillary flange (bifid),
 26. *Lacrimal orbital rim
 - (0) lacrimal crest absent
 - (1) partially developed lacrimal crest
 - (2) fully developed lacrimal crest,
 27. *Antorbital fossa
 - (0) antorbital fossa absent
 - (1) weak or partial fossa development
 - (2) very deep antorbital fossa,
 28. *Orbitosphenoid
 - (0) orbitosphenoid identifiable in lateral view as a large ossification
 - (1) orbitosphenoid identifiable in lateral view as a small ossification
 - (2) orbitosphenoid is very small or absent and not obvious in lateral view,
 29. Alisphenoid
 - (0) alisphenoid-parietal contact
 - (1) squamosal-frontal contact ,
 30. *Sphenorbital fissure and foramen rotundum
 - (0) sphenorbital fissure slightly larger than foramen rotundum. Both canals are tube-

- like in shape, especially the foramen rotundum
 (1) sphenorbital fissure is enlarged and more widely open, and there is a reduction in the length of the tube leading to the foramen rotundum
 (2) sphenorbital fissure is further enlarged and open, and there is no tube leading to the foramen rotundum, which instead appears,
31. Presence of Accessory fenestrae
 (0) absent
 (1) present,
32. Presence of dividing septa in maxillopalatine fenestrae
 (0) septum present in maxillopalatine fenestrae
 (1) septum absent in maxillopalatine fenestrae,
33. Postglenoid foramen
 (0) foramen bound by squamosal or squamosal and alisphenoid
 (1) foramen bounded medially by the petrosal,
34. Morphology of the primary foramen ovale
 (0) primary foramen ovale is between alisphenoid and petrosal
 (1) primary foramen ovale is entirely within the alisphenoid,
35. *Morphology of the secondary foramen ovale
 (0) secondary foramen ovale absent
 (1) secondary foramen ovale defined by a complete strut or bridge formed by the alisphenoid, but the primary foramen ovale is still visible
 (2) secondary foramen ovale present, and extensive ossification of the alisphenoid means that the primary foramen ovale is no longer visible in intact skulls,
36. *Morphology of the ectotympanic
 (0) thin
 (1) somewhat thickened
 (2) further thickened
 (3) heavily thickened,
37. *Degree of inflation of the alisphenoid tympanic process
 (0) alisphenoid tympanic process small, lateral and medial walls open.
 (1) alisphenoid tympanic process largely open but medial wall enclosed greater than in state 0, and hypotympanic sinus is also enlarged relative to state 0
 (2) alisphenoid tympanic process and hypotympanic sinus further enlarged relative to state 1; hypotympanic sinus walled posteriorly by the alisphenoid
 (3) alisphenoid tympanic process and hypotympanic sinus greatly hypertrophied,
38. Alisphenoid tympanic process shape
 (0) flattened
 (1) ventrally rounded, anterior boundary rounded does not extend as far as the transverse foramen or foramen ovale
 (2) ventrally rounded, anterior boundary pointed and extends as far as the transverse foramen
 (3) ventrally angular, anterior boundary pointed and terminates anterior to the transverse foramen,
39. *Morphology of the rostral tympanic process of the petrosal
 (0) rostral tympanic process of the petrosal absent or very small
 (1) rostral tympanic process of the petrosal forms a distinct projecting process that partially walls the posteromedial margin of the hypotympanic sinus .
 (2) rostral tympanic process of the petrosal further enlarged, forming elongate crestlike process that extends the length of the promontorium and forms posteromedial wall of the hypotympanic sinus; medial margin of petrosal overlaps basioccipital.
 (3) ventral margin of the rostral tympanic process of the petrosal extends laterally and slightly dorsally, resulting in the formation of a distinct hypotympanic sinus within the rostral tympanic process itself
 (4) dorsal extension of the ventral margin of the rostral tympanic process relative to state 3, resulting in lateral wall to the hypotympanic sinus within the process ,
40. Epitympanic recess

- (0) poorly defined and shallow
 (1) wider and deeper than the plesiomorphic state but still relatively poorly defined
 (2) deep sinus with enclosing walls that is well distinguished from remainder of auditory cavity
 (3) wide and deep sinus that extends posterolaterally,
41. Squamosal epitympanic sinus
 (1) absent
 (2) present, poorly defined
 (3) wide with high posterior wall
 (4) deep and round,
42. Supraoccipital shape
 (0) supraoccipital about as tall as it is wide
 (1) supraoccipital taller than it is wide ,
43. Postorbital processes
 (0) absent or indistinct
 (1) present,
44. Left and right parietal suture
 (0) median suture present
 (1) partially or completely co-ossified suture,
45. *Sagittal crest
 (0) no sagittal crest
 (1) sagittal crest small, not extending to frontals
 (0) sagittal crest large and extending to frontals,
46. Interparietal
 (0) absent
 (1) present,
47. Lambdoid sesamoids
 (0) absent
 (1) present,
48. *Number of mental foramen
 (0) one mental foramen
 (1) two mental foramina
 (2) three or more mental foramina,
49. Shape of I1
 (0) styliform or chisellike
 (1) mesiodistally expanded and flat-crowned,
50. Upper canine alveolus
 (0) occupies premaxillary-maxillary suture
 (1) entirely contained within maxillary,
51. *Relative height of P2 and P3
 (0) P2 taller than P3
 (1) P2 and P3 subequal in height
 (2) P3 taller than P2,
52. Posterior crest of P3
 (0) well-developed posterior cutting edge
 (1) lacking posterior cutting edge,
53. *Relative height of p2 and p3
 (0) p2 taller than p3
 (1) p2 and p3 subequal in height
 (2) p3 taller than p2,
54. Hypoconulid notch
 (0) present in anterior cingulum of m2-4
 (1) absent,
55. *Relative position of hypoconid to protoconid on m3
 (0) buccally salient to protoconid
 (1) subequal to protoconid
 (2) lingual to salient protoconid,
56. Posterior cingulid
 (0) absent
 (1) present,
57. Shape of narial flange of premaxilla
 (0) no distinct process
 (1) wing-like narial processes present,
58. Position of lacrimal foramen
 (0) within lacrimal
 (1) within lacrimal-maxillary suture,
59. Supraoccipital contribution to foramen magnum
 (0) contributes to superior margin of foramen magnum
 (1) exoccipitals contact each other medially, excluding the supraoccipital from the foramen magnum ,
60. Shape of I2-4
 (0) rhomboidal crowns
 (1) mesiodistally expanded and flat-crowned,
61. Shape of upper canine
 (0) single-rooted unicuspid upper canine
 (1) accessory cusps are present on either side of the major cusp of C1,
62. Lower molar crown height
 (0) lower molars are as high on the buccal side as they are on the lingual side

- (1) lower molar height is significantly higher on buccal side than lingual side,
63. Position of the metacone
 (0) metacone is directly posterior to the paracone
 (1) metacone is shifted lingually in relation to the paracone,
64. Size of I3
 (0) I2-4 are the same size
 (1) I3 is larger than I2 and I4,
65. Lingual cusp presence on lower incisors
 (0) present
 (1) absent,
66. Diastema between i3 and canine
 (0) no diastema
 (1) diastema present,
67. Shape of lower canine
 (0) single-rooted unicuspid lower canine
 (1) accessory cusps are present on either side of the major cusp of c1,
68. Size of upper or lower canine
 (0) large, raised above premolars
 (1) small, about as high as premolars,
69. *Diastema between C1 and P1
 (0) no diastema
 (1) short, less than the length of P1
 (0) long, more than the length of P1,
70. *Length of P1
 (0) P1 is shorter than P2
 (1) P1 is as long as P2
 (2) P1 is longer than P2,
71. Anterior cusp of P1 and/or P2
 (0) tall distinct cusp
 (1) small remnant or no cusp,
72. *Diastema between P1 and P2
 (0) no diastema
 (1) short, less than the length of p1
 (2) long, more than the length of p1,
73. Morphology of the central cusp of P1 and P2
 (0) central cusp is not inflated
 (1) central cusp is inflated widening the tooth anteriorly,
74. *Relative length of P2 and P3
 (0) P3 almost twice as long as P2
 (1) P2 shorter than P3
- (2) P2 and P3 subequal length
 (3) P2 longer than P3
 (4) P2 twice as long as P3,
75. *Diastema between canine and p1
 (0) no diastemata
 (1) short, less than the length of p1
 (2) long, more than the length of p1,
76. Length of p1
 (0) p1 is shorter than either p2 or p3
 (1) p1 is as long as p2 or p3,
77. Anterior cusp of p1
 (0) tall distinct cusp
 (1) none or small remnant,
78. Anterior cusp of p2
 (0) tall distinct cusp
 (1) none or small remnant,
79. *Diastema between p1 and p2
 (0) no diastemata
 (1) short, less than the length of p1
 (2) long, more than the length of p1,
80. *Relative length of p2 and p3
 (0) p3 almost twice as long as p2
 (1) p2 shorter than p3
 (2) p2 and p3 subequal length
 (3) p2 longer than P3,
81. Anterior cusp of p3
 (0) tall distinct cusp
 (1) none or small remnant,
82. p3 major cusp development
 (0) p3 major cusp laterally compressed
 (1) p3 major cusp very large,
83. Reclining of p3
 (0) the anterior and posterior roots of p3 are level
 (1) the anterior root of p3 is more exposed than the posterior root, reclining p3 toward m1,
84. *Size of StA on M1
 (0) StA is large, with a long crest running anteroposteriorly
 (1) StA is small, with a short or no crest running anteroposteriorly
 (2) StA remnant or no StA,
85. Morphology of StB/StC on M1
 (0) no StC or B
 (1) StB and StC are distinct cusps

- (2) StB and StC are fused and oval in shape connected by a stylar crest but clearly identifiable as separate cusp
 (3) StB and StC are fused and oval in shape connected by a stylar crest but difficult to clearly identify each cusp,
86. *Relative size of StB and StC on M1
 (0) StB larger than StC
 (1) StB subequal to StC
 (2) StC larger than StB,
87. Connection of StB and StD on M1
 (0) StB/C and StD are connected by a series of crests
 (1) StB/C and StD are not connected by any crests,
88. *Posterior cingulum of M1
 (0) absent
 (1) present
 (2) present and wide,
89. *Termination of postprotocrista on M1
 (0) postprotocrista ends on anterior flank of metacone
 (1) postprotocrista ends on lingual flank of metacone
 (2) postprotocrista ends on posterolingual flank of metacone
 (3) postprotocrista joins with the posterior cingulum and ends posteriorly to the midpoint of the postmetacrista
 (4) postprotocrista joins with the posterior cingulum and ends at the lingual flank of the metastylar tip,
90. *Position of metaconule on M1
 (0) metaconule is directly positioned at the base of the metacone
 (1) a small shelf is between the base of the metacone and the metaconule
 (2) a larger shelf is between the base of the metacone and the metaconule,
91. StD1 on M1
 (0) present
 (1) absent,
92. *StE on M1
 (0) StE present as a distinct cusp
 (1) remnant of StE as a stylar crest or small cusp
 (2) no StE (no stylar crest),
93. *Anterior cingulum of M2
 (0) no anterior cingulum
 (1) small anterior cingulum lingual to anterior tip of tooth
 (2) small anterior cingulum connected to protocone shelf by a small shelf
 (3) large anterior cingulum expanded further up to the protocone,
94. *Size of StA on M2
 (0) StA is large, with a long crest running anteroposteriorly
 (1) StA is small, with a short or no crest running anteroposteriorly
 (2) no StA,
95. Morphology of StB on M2
 (0) StB is oval with a stylar crest running through it
 (1) StB is conical with no stylar crest connection,
96. Connection of StB and StD on M2
 (0) StB and StD are connected by a series of crests
 (1) StB and StD are not connected by any crests,
97. *Direction of preparacrista of M2
 (0) preparacrista terminates at base of StB (no crest connection).
 (1) preparacrista terminates at the tip StB.
 (2) preparacrista connects to StB with a weak connection to StA
 (3) preparacrista connects to parastylar tip/StA,
98. *Stylar crest on M2
 (0) stylar crest present on StD connects to metastylar tip
 (1) StD is a conical cusp not connected to the stylar crest running to the metastylar tip
 (2) StD is a conical cusp and no stylar crest present,
99. *Posterior cingulum of M2
 (0) absent
 (1) present
 (2) present and wide,
100. *Termination of postprotocrista on M2
 (0) postprotocrista ends on anterior flank of metacone

- (1) postprotocrista ends on lingual flank of metacone
 - (2) postprotocrista ends on posterolingual flank of metacone
 - (3) postprotocrista joins with the posterior cingulum and ends posteriorly to the midpoint of the postmetacrista
 - (4) postprotocrista joins with the posterior cingulum and ends at the lingual flank of the metastylar tip,
101. *Position of metaconule on M2
- (0) metaconule is directly positioned at the base of the metacone
 - (1) a small shelf is between the base of the metacone and the metaconule
 - (2) a larger shelf is between the base of the metacone and the metaconule,
102. *StC on M2
- (0) present as tall cusp
 - (1) small remnant present
 - (2) absent,
103. StD1 on M2
- (0) present
 - (1) absent,
104. *StE on M2
- (0) StE present as a distinct cusp
 - (1) remnant of StE as a stylar crest
 - (2) no StE (no stylar crest),
105. *Size of StA on M3
- (0) StA is large, with a long crest running anteroposteriorly
 - (1) StA is small, with a short or no crest running anteroposteriorly
 - (2) no St,
106. Morphology of StB on M3
- (0) StB is oval with a stylar crest running through it
 - (1) StB is conical with no stylar crest connection (except by wear),
107. Connection of StB and StD on M3
- (0) StB and StD are connected by a series of crests
 - (1) StB and StD are not connected by any crests,
108. *Direction of preparacrista of M3
- (0) preparacrista terminates at base of StB (no crest connection).
 - (1) preparacrista terminates at the tip StB.
 - (2) preparacrista connects a crest linking StA and StB
 - (3) preparacrista connects to parastylar tip/ StA,
109. *Stylar crest on M3
- (0) stylar crest present on StD connects to metastylar tip
 - (1) StD is a conical cusp not connected to the stylar crest running to the metastylar tip
 - (2) StD is a conical cusp and no stylar crest present,
110. *Termination of postprotocrista/ posthypocrista on M3
- (0) postprotocrista ends on anterior flank of metacone
 - (1) postprotocrista ends on lingual flank of metacone
 - (2) postprotocrista ends on posterolingual flank of metacone
 - (3) postprotocrista joins with the posterior cingulum and ends posteriorly to the midpoint of the postmetacrista
 - (4) postprotocrista joins with the posterior cingulum and ends at the lingual flank of the metastylar tip,
111. *Position of metaconule on M3
- (0) metaconule is directly positioned at the base of the metacone
 - (1) a small shelf is between the base of the metacone and the metaconule
 - (2) a larger shelf is between the base of the metacone and the metaconule,
112. *StC on M3
- (0) present as tall cusp
 - (1) small remnant present
 - (2) absent,
113. StD1 on M3
- (0) present
 - (1) absent,
114. *StE on M3
- (0) StE present as a distinct cusp
 - (1) remnant of StE as a stylar crest
 - (2) no StE (no stylar crest),
115. *Anterior cingulum of M4
- (0) no anterior cingulum

- (1) small anterior cingulum lingual to anterior tip of tooth
 (2) small anterior cingulum connected to protocone shelf by a small shelf
 (3) large anterior cingulum expanded further up to the protocone,
116. *StB on M4
 (0) no StB
 (1) small StB
 (2) Large StB,
117. Connection of StA and StB on M4
 (0) no connection
 (1) crest connecting the two cusps,
118. Direction of preparacrista of M4
 (0) preparacrista terminates StA
 (1) preparacrista terminates at the anterior flank of StB,
119. Postparacrista of M4
 (0) postparacrista straight
 (1) postparacrista curves as a small centrocrista and ends just after the centrocrista,
120. *Termination of postprotocrista on M4
 (0) postprotocrista ends anterior to the most posterior end of the postparacrista
 (1) postprotocrista ends level with the most posterior end of the postparacrista
 (2) postprotocrista ends posterior to the most posterior end of the postparacrista ,
121. *Metacone on M4
 (0) absent
 (1) small metacone raise above the postparacrista
 (2) large metacone expands the length of the tooth,
122. StC/D on M4
 (0) absent
 (1) present,
123. Presence of protocone on M4
 (0) present
 (1) absent,
124. Anterior cingulid on m1
 (0) absent or small remnant
 (1) present,
125. Hypoflexid on m1
 (0) absent
 (1) present,
126. *Shape of trigonid on m1
 (0) paraconid-metaconid distance is longer than metaconid-protoconid distance
 (1) paraconid-metaconid distance is as long as metaconid-protoconid distance
 (0) paraconid-metaconid distance is shorter than metaconid-protoconid distance
 (1) paraconid highly reduced or absent,
127. Position of paraconid on m1
 (0) paraconid anterior to metaconid
 (1) paraconid anterobuccal to metaconid,
128. Shape of unworn entoconid on m1-3
 (0) oval
 (1) triangular (wider posteriorly than anteriorly)
 (2) conical,
129. *Cristid obliqua termination on m1
 (0) cristid obliqua terminates buccal to level with the protocone
 (1) cristid obliqua terminates lingual to the protocone to the midpoint to the tooth width
 (2) cristid obliqua terminates lingual to the midpoint of the tooth width,
130. Posthypocristid direction on m1
 (0)oblique to the tooth row axis
 (1) perpendicular to the tooth row axis ,
131. Connection of posthypocristid on m1
 (0) posthypocristid connects to hypoconulid
 (1) posthypocristid connects to base of entoconid when the tooth is unworn, but as the tooth wears down, a crest connects the tip of the entoconid to the posthypocristid.,
132. Size of hypoconulid on m1
 (0) large distinct cusp
 (1) small cusp,
133. *Shape of trigonid on m2
 (0) paraconid-metaconid distance is longer than metaconid-protoconid distance
 (1) paraconid-metaconid distance is as long as metaconid-protoconid distance
 (2) paraconid-metaconid distance is shorter than metaconid-protoconid distance
 (3) paraconid highly reduced or absent,

134. *Cristid obliqua termination on m2
 (0) cristid obliqua terminates buccal to the protocone
 (1) cristid obliqua terminates lingual to the protocone about midpoint to the tooth width
 (2) cristid obliqua terminates lingual to the midpoint of the tooth width,
135. Posthypocristid direction on m2
 (0) oblique to the tooth row axis
 (1) perpendicular to the tooth row axis ,
136. Connection of posthypocristid on m2
 (0) posthypocristid connects to hypoconulid
 (1) posthypocristid connects to entoconid,
137. *Size of hypoconulid on m2
 (0) large distinct cusp
 (1) small cusp
 (2) hypoconulid absent,
138. *Shape of trigonid on m3
 (0) paraconid-metaconid distance is longer than metaconid-protoconid distance
 (1) paraconid-metaconid distance is as longer as metaconid-protoconid distance
 (2) paraconid-metaconid distance is shorter than metaconid-protoconid distance
 (3) paraconid highly reduced or absent,
139. *Cristid obliqua termination on m3
 (0) cristid obliqua terminates buccal to the protocone
 (1) cristid obliqua terminates lingual to the protocone about midpoint to the tooth width
 (2) cristid obliqua terminates lingual to the midpoint of the tooth width,
140. Posthypocristid direction on m3
 (0) oblique to the tooth row axis
 (1) perpendicular to the tooth row axis ,
141. Connection of posthypocristid on m3
 (0) posthypocristid connects to hypoconulid
 (1) posthypocristid connects to entoconid,
142. *Size of hypoconulid on m3
 (0) large distinct cusp
 (1) small cusp
 (2) hypoconulid absent,
143. *Shape of trigonid on m4
 (0) paraconid-metaconid distance is longer than metaconid-protoconid distance
 (1) paraconid-metaconid distance is as longer as metaconid-protoconid distance
 (2) paraconid-metaconid distance is shorter than metaconid-protoconid distance
 (3) paraconid highly reduced or absent,
144. Preentocristid on m4
 (0) present
 (1) absent,
145. Preentocristid orientation on m4
 (0) anteroposterior
 (1) oblique,
146. Postentocristid on m4
 (0) absent
 (1) present,
147. Postentocristid orientation on m4
 (0) anteroposterior
 (1) oblique,
148. Cristid obliqua termination on m4
 (0) cristid obliqua terminates lingual to the protocone about midpoint to the tooth width
 (1) cristid obliqua terminates lingual to the midpoint of the tooth width,
149. *Posthypocristid direction on m4
 (0) oblique to the tooth row axis
 (1) perpendicular to the tooth row axis
 (2) anteriorly orientated,
150. *Size of entoconid
 (0) large distinct cusp
 (1) small cusp
 (2) entoconid absent,
151. *Size of hypoconulid on m4
 (0) large distinct cusp
 (1) small cusp
 (2) hypoconulid absent,
152. Buccal shelf on m4
 (0) buccal shelf end at buccal side of hypoconid
 (1) buccal shelf buccally reduced (hypoconid more buccal than shelf),
153. Presence of P3
 (0) present
 (1) absent,

- | | |
|-------------------------------------|--------------------------------------|
| 154. Presence of p3 | (1) present, |
| (0) present | 156. Presence of maxillary fenestrae |
| (1) absent, | (0) absent |
| 155. Presence of palatine fenestrae | (1) present, |
| (0) absent | |

APPENDIX 2

Nexus-formatted character matrix for the 42 taxa included in our phylogenetic analyses. Outgroup taxa were *Djarthia murgonensis*, *Barinya wangala*, *Mutpuracinus archibaldi*, *Dasyurus hallucatus*, *Dasyuroides byrnei*, *Phascogale tapoatafa*, *Antechinus stuartii*, *Sminthopsis macroura*. ? = missing data; - = inapplicable.

```
#NEXUS
```

```
BEGIN TAXA;
  DIMENSIONS NTAX=42;
  TAXLABELS
    'D. murgonensis'
    'M. archibaldi'
    'B. wangala'
    'D. hallucatus'
    'D. byrnei'
    'P. tapoatafa'
    'A. stuartii'
    'S. macroura'
    'C. ecaudatus'
    'M. lagotis'
    'M. leucura'
    'I. australis'
    'P. broadbenti'
    'P. raffrayana'
    'M. longicauda'
    'M. papuensis'
    'R. prattorum'
    'E. clara'
    'E. davidi'
    'E. kalubu'
    'E. rufescens'
    'cf. P. tedfordi'
    'cf. P. sp.'
    'I. auratus'
    'I. obesulus'
    'I. macrourus'
    'P. nasuta'
    'P. bougainville'
    'P. gunnii'
    'P. eremiana'
    'P. sobbei'
    'P. bowensis'
    'P. allinghamensis'
    'Y. burchfieldi'
    'Y. kida'
    'G. speciosus'
    'G. grandis'
    'G. amplus'
```

```

      'G. adversus'
      'B. palara'
      'B. muirheadae'
      'B. campbelli'
    ;
ENDBLOCK;
BEGIN CHARACTERS;
  DIMENSIONS NCHAR=156;
  FORMAT DATATYPE=STANDARD MISSING=? GAP=- SYMBOLS="01234";
  CHARLABELS
    [1] 'Upper incisor number'
    [2] 'Diastema between I4 and I5'
    [3] 'I5 morphology'
    [4] 'Degree of development of lingual shelf on P3'
    [5] 'P3 major cusp development'
    [6] 'Stylar crest on M1'
    [7] 'Anterior cingulum of M1'
    [8] 'Anterior cingulum of M3'
    [9] 'Direction of preparacrista of M1'
    [10] 'Posterior cingulum of M3'
    [11] 'Morphology of the centrocrista on M1 and M2'
    [12] 'Morphology of centrocrista on M3'
    [13] 'Lobation of i3'
    [14] 'Length of p3'
    [15] 'Presence of preentocristid'
    [16] 'Direction of preentocristid of m1-3'
    [17] 'Cusp within the hypoflexid region, between the talonid
and trigonid on the buccal side'
    [18] 'Distinction between lower molar crowns and roots'
    [19] 'Hypoconulid posterior to entoconid'
    [20] 'Size of talonid on m4'
    [21] 'Snout length and premaxilla size'
    [22] 'Width of nasals'
    [23] 'Position of nasal-frontal suture/maximum posterior
extension of nasals'
    [24] 'Infraorbital canal length'
    [25] 'Jugal-maxilla contact'
    [26] 'Lacrimal orbital rim'
    [27] 'Antorbital fossa'
    [28] Orbitosphenoid
    [29] Alisphenoid
    [30] 'Sphenorbital fissure and foramen rotundum'
    [31] 'Presence of Accessory fenestrae'
    [32] 'Presence of dividing septa in maxillopalatine fenestrae'
    [33] 'Postglenoid foramen'
    [34] 'Morphology of the primary foramen ovale'
    [35] 'Morphology of the secondary foramen ovale'
    [36] 'Morphology of the ectotympanic'
    [37] 'Degree of inflation of the alisphenoid tympanic process'
    [38] 'Alisphenoid tympanic process shape'
    [39] 'Morphology of the rostral tympanic process of the
petrosal'

```

- [40] 'Epitympanic recess'
- [41] 'Squamosal epitympanic sinus'
- [42] 'Supraoccipital shape'
- [43] 'Postorbital processes'
- [44] 'Left and right parietal suture'
- [45] 'Sagittal crest'
- [46] Interparietal
- [47] 'Lambdoid sesamoids'
- [48] 'Number of mental foramen'
- [49] 'Shape of I1'
- [50] 'Upper canine alveolus'
- [51] 'Relative height of P2 and P3'
- [52] 'Posterior crest of P3'
- [53] 'Relative height of p2 and p3'
- [54] 'Hypoconulid notch'
- [55] 'Relative position of hypoconid to protoconid on m3'
- [56] 'Posterior cingulid'
- [57] 'Shape of narial flange of premaxilla'
- [58] 'Position of lacrimal foramen'
- [59] 'Supraoccipital contribution to foramen magnum'
- [60] 'Shape of I2-4'
- [61] 'Shape of upper canine'
- [62] 'Lower molar crown height'
- [63] 'Position of the metacone'
- [64] 'Size of I3'
- [65] 'Lingual cusp presence on lower incisors'
- [66] 'Diastema between i3 and canine'
- [67] 'Shape of lower canine'
- [68] 'Size of upper or lower canine'
- [69] 'Diastema between C1 and P1'
- [70] 'Length of P1'
- [71] 'Anterior cusp of P1 and/or P2'
- [72] 'Diastema between P1 and P2'
- [73] 'Morphology of the central cusp of P1 and P2'
- [74] 'Relative length of P2 and P3'
- [75] 'Diastema between canine and p1'
- [76] 'Length of p1'
- [77] 'Anterior cusp of p1'
- [78] 'Anterior cusp of p2'
- [79] 'Diastema between p1 and p2'
- [80] 'Relative length of p2 and p3'
- [81] 'Anterior cusp of p3'
- [82] 'p3 major cusp development'
- [83] 'Reclining of p3'
- [84] 'Size of StA on M1'
- [85] 'Morphology of StB/C on M1'
- [86] 'Relative size of StB and StC on M1'
- [87] 'Connection of StB and StD on M1'
- [88] 'Posterior cingulum of M1'
- [89] 'Termination of postprotocrista on M1'
- [90] 'Position of metaconule on M1'
- [91] 'StD1 on M1'

- [92] 'StE on M1'
- [93] 'Anterior cingulum of M2'
- [94] 'Size of StA on M2'
- [95] 'Morphology of StB on M2'
- [96] 'Connection of StB and StD on M2'
- [97] 'Direction of preparacrista of M2'
- [98] 'Stylar crest on M2'
- [99] 'Posterior cingulum of M2'
- [100] 'Termination of postprotocrista on M2'
- [101] 'Position of metaconule on M2'
- [102] 'StC on M2'
- [103] 'StD1 on M2'
- [104] 'StE on M2'
- [105] 'Size of StA on M3'
- [106] 'Morphology of StB on M3'
- [107] 'Connection of StB and StD on M3'
- [108] 'Direction of preparacrista of M3'
- [109] 'Stylar crest on M3'
- [110] 'Termination of postprotocrista/posthypocrista on M3'
- [111] 'Position of metaconule on M3'
- [112] 'StC on M3'
- [113] 'StD1 on M3'
- [114] 'StE on M3'
- [115] 'Anterior cingulum of M4'
- [116] 'StB on M4'
- [117] 'Connection of StA and StB on M4'
- [118] 'Direction of preparacrista of M4'
- [119] 'Postparacrista of M4'
- [120] 'Termination of postprotocrista on M4'
- [121] 'Metacone on M4'
- [122] 'StC/D on M4'
- [123] 'Presence of protocone on M4'
- [124] 'Anterior cingulid on m1'
- [125] 'Hypoflexid on m1'
- [126] 'Shape of trigonid on m1'
- [127] 'Position of paraconid on m1'
- [128] 'Shape of unworn entoconid on m1-3'
- [129] 'Cristid obliqua termination on m1'
- [130] 'Posthypocristid direction on m1'
- [131] 'Connection of posthypocristid on m1'
- [132] 'Size of hypoconulid on m1'
- [133] 'Shape of trigonid on m2'
- [134] 'Cristid obliqua termination on m2'
- [135] 'Posthypocristid direction on m2'
- [136] 'Connection of posthypocristid on m2'
- [137] 'Size of hypoconulid on m2'
- [138] 'Shape of trigonid on m3'
- [139] 'Cristid obliqua termination on m3'
- [140] 'Posthypocristid direction on m3'
- [141] 'Connection of posthypocristid on m3'
- [142] 'Size of hypoconulid on m3'
- [143] 'Shape of trigonid on m4'

```

[144] 'Preentocristid on m4'
[145] 'Preentocristid orientation on m4'
[146] 'Postentocristid on m4'
[147] 'Postentocristid orientation on m4'
[148] 'Cristid obliqua termination on m4'
[149] 'Posthypocristid direction on m4'
[150] 'Size of entoconid'
[151] 'Size of hypoconulid on m4'
[152] 'Buccal shelf on m4'
[153] 'Presence of P3'
[154] 'Presence of p3'
[155] 'Presence of palatine fenestrae'
[156] 'Presence of maxillary fenestrae'
;
STATELABELS
1
    'five incisors present'
    'four incisors present (I5 lost)',
2
    'absent'
    'present',
3
    'I5 similar in morphology to I1-4'
    'I5 pointed and strongly canine-like'
    'I5 is premolar like',
4
    'no shelf'
    'small/weakly developed shelf'
    'well-developed lingual shelf'
    'well-developed lingual shelf that extends to the buccal
side of P3',
5
    'P3 major cusp laterally compressed'
    'P3 major cusp laterally enlarged but not conical'
    'P3 major cusp large and conical, but P3 is narrower than
M1'
    'P3 Major cusp large and conical, and P3 is wider than
M1',
6
    'stylar crest present on StD connects to metastylar tip'
    'StD is a conical cusp not connected to the stylar crest
running to the metastylar tip'
    'StD is a conical cusp and no stylar crest present',
7
    'no anterior cingulum'
    'small anterior cingulum lingual to anterior tip of
tooth, no connection to talon'
    'anterior cingulum enlarged and connects to talon as
small shelf',
8
    'no anterior cingulum'

```

tooth' 'small anterior cingulum lingual to anterior tip of
 a small shelf' 'small anterior cingulum connected to protocone shelf by
 protocone', 'large anterior cingulum expanded further up to the
 9 'preparacrista anterobuccally orientated to connect to
 anteriorly positioned StB'
 'preparacrista buccally orientated (perpendicular to
 tooth row) then posterobuccally orientated'
 'preparacrista posterobuccally orientated to connect to
 posteriorly located StB'
 'preparacrista posterobuccally orientated to connect to
 StB and then reconnects with postparacrista posteriorly',
 10
 'absent'
 'present'
 'present and wide',
 11
 'postparacrista and premetacrista contact each other,
 forming a complete centrocrista that connects the paracone and metacone
 (more lingually)'
 'postparacrista and premetacrista contact each other,
 forming a complete centrocrista that connects the paracone and metacone
 (more buccally)'
 'postparacrista does not connect to the premetacrista and
 ends at the base of StB, premetacrista ends at base of StD',
 12
 'postparacrista and premetacrista contact each other,
 forming a complete centrocrista that connects the paracone and metacone
 (more lingually)'
 'postparacrista and premetacrista contact each other,
 forming a complete centrocrista that connects the paracone and metacone
 (more buccally)'
 'postparacrista does not connect to the premetacrista and
 ends at the base of StB, premetacrista ends at base of StD',
 13
 'i3 is unicuspid'
 'i3 posterior cusp present but small'
 'I3 posterior cusp present and large',
 14
 'p3 longer or equal in length to p2 '
 'p3 shorter than p2 ',
 15
 'present'
 'absent',
 16
 'anteroposterior'
 'oblique',
 17
 'no median buccal cusp present'

18 'median buccal cusp present',
 'crown distinct from roots'
 enamel)',
 19 'crown and root indistinct (other than for limit of
 entoconid',
 20 'hypoconulid positioned posterobuccal to the entoconid'
 'hypoconulid positioned almost directly posterior to the
 entoconid and hypoconid large, talonid relatively wide,
 crests clearly identifiable'
 'entoconid and hypoconid smaller than in state 0, talonid
 smaller'
 'further reduction of entoconid and hypoconid, talonid
 very small, crest poorly defined',
 21 'premaxilla taller than it is long; maxilla-nasal contact
 longer than premaxilla-nasal contact (usually correlated with a relatively
 short snout)'
 'premaxilla longer than it is tall; premaxilla-nasal
 contact longer than maxilla-nasal contact (usually correlated with a
 relatively elongate snout)',
 22 'broad nasals'
 'slender nasals, not markedly expanded posteriorly',
 23 'posterior to the anterior rim of the orbit when viewed
 laterally'
 'nasals terminate just anterior to the orbit when viewed
 laterally(associated with a wide maxilla-frontal suture)'
 'nasals terminate well anterior to the anterior margin of
 the orbit',
 24 'long infraorbital canal (longer than half the molar
 row)'
 'short infraorbital canal (shorter or equal to half the
 molar row)',
 25 'jugal invades the maxilla and extends onto the facial
 region of the skull (not bifid)'
 'maxilla invades the zygomatic arch so that the jugal has
 two thin wings around the posterior maxillary flange (bifid)',
 26 'lacrimal crest absent'
 'partially developed lacrimal crest'
 'fully developed lacrimal crest',
 27 'antorbital fossa absent'
 'weak or partial fossa development'
 'very deep antorbital fossa',
 28

ossification' 'orbitosphenoid identifiable in lateral view as a large
 ossification' 'orbitosphenoid identifiable in lateral view as a small
 lateral view', 'orbitosphenoid is very small or absent and not obvious in
 29
 'alisphenoid-parietal contact'
 'squamosal-frontal contact',
 30
 'sphenorbital fissure slightly larger than foramen
 rotundum. Both canals are tubelike in shape, especially the foramen
 rotundum'
 'sphenorbital fissure is enlarged and more widely open,
 and there is a reduction in the length of the ''tube'' leading to the
 foramen rotundum'
 'sphenorbital fissure is further enlarged and open, and
 there is no ''tube'' leading to the foramen rotundum, which instead
 appears',
 31
 'absent'
 'present',
 32
 'septum present in maxillopalatine fenestrae'
 'septum absent in maxillopalatine fenestrae',
 33
 'foramen bound by squamosal or squamosal and alisphenoid'
 'foramen bounded medially by the petrosal',
 34
 'primary foramen ovale is between alisphenoid and
 petrosal'
 'primary foramen ovale is entirely within the
 alisphenoid',
 35
 'secondary foramen ovale absent'
 'secondary foramen ovale defined by a complete strut or
 bridge formed by the alisphenoid, but the primary foramen ovale is still
 visible'
 'secondary foramen ovale present, and extensive
 ossification of the alisphenoid means that the primary foramen ovale is no
 longer visible in intact skulls',
 36
 'thin'
 'somewhat thickened'
 'further thickened'
 'heavily thickened',
 37
 'alisphenoid tympanic process small, lateral and medial
 walls open'
 'alisphenoid tympanic process largely open but medial
 wall enclosed greater than in state 0, and hypotympanic sinus is also
 enlarged relative to state 0'

'alisphenoid tympanic process and hypotympanic sinus further enlarged relative to state 1; hypotympanic sinus walled posteriorly by the alisphenoid'

'alisphenoid tympanic process and hypotympanic sinus greatly hypertrophied',

38

'flattened'

'ventrally rounded, anterior boundary rounded does not extend as far as the transverse foramen or foramen ovale'

'ventrally rounded, anterior boundary pointed and extends as far as the transverse foramen'

'ventrally angular, anterior boundary pointed and terminates anterior to the transverse foramen',

39

'rostral tympanic process of the petrosal absent or very small'

'rostral tympanic process of the petrosal forms a distinct projecting process that partially walls the posteromedial margin of the hypotympanic sinus'

'rostral tympanic process of the petrosal further enlarged, forming elongate crestlike process that extends the length of the promontorium and forms posteromedial wall of the hypotympanic sinus; medial margin of petrosal overlaps basioccipital'

'ventral margin of the rostral tympanic process of the petrosal extends laterally and slightly dorsally, resulting in the formation of a distinct hypotympanic sinus within the rostral tympanic process itself'

'further dorsal extension of the ventral margin of the rostral tympanic process relative to state 3, resulting in lateral wall to the hypotympanic sinus within the process',

40

'poorly defined and shallow'

'wider and deeper than the plesiomorphic state but still relatively poorly defined'

'deep sinus with enclosing walls that is well distinguished from remainder of auditory cavity'

'wide and deep sinus that extends posterolaterally',

41

'absent'

'present, poorly defined'

'wide with high posterior wall'

'deep and round',

42

'supraoccipital about as tall as it is wide'

'supraoccipital taller than it is wide',

43

'absent or indistinct'

'present',

44

'median suture present'

'partially or completely co-ossified suture',

45

'no sagittal crest'
 'sagittal crest small, not extending to frontals'
 'sagittal crest large and extending to frontals',
 46
 'absent'
 'present',
 47
 'absent'
 'present',
 48
 'one mental foramen'
 'two mental foramina'
 'three or more mental foramina',
 49
 'styliiform or chisel-like'
 'mesiodistally expanded and flat-crowned',
 50
 'occupies premaxillary-maxillary suture'
 'entirely contained within maxillary',
 51
 'P2 taller than P3'
 'P2 and P3 subequal in height'
 'P3 taller than P2',
 52
 'well-developed posterior cutting edge'
 'lacking posterior cutting edge',
 53
 'p2 taller than p3'
 'p2 and p3 subequal in height'
 'p3 taller than p2',
 54
 'present in anterior cingulum of m2-4'
 'absent',
 55
 'buccally salient to protoconid'
 'subequal to protoconid'
 'lingual to salient protoconid',
 56
 'absent'
 'present',
 57
 'no distinct process'
 ''wing-like'' narial processes present',
 58
 'within lacrimal'
 'within lacrimal-maxillary suture',
 59
 'contributes to superior margin of foramen magnum'
 'exoccipitals contact each other medially, excluding the
 supraoccipital from the foramen magnum',
 60
 'rhomboidal crowns'

61 'mesiodistally expanded and flat-crowned',
 'single-rooted unicuspid upper canine'
 cusp of C1', 'accessory cusps are present on either side of the major
 62
 'lower molars are as high on the buccal side as they are
 on the lingual side'
 'lower molar height is significantly higher on buccal
 side than lingual side',
 63
 'metacone is directly posterior to the paracone'
 paracone', 'metacone is shifted lingually in relation to the
 64
 'I2-4 are the same size'
 'I3 is larger than I2 and I4',
 65
 'present'
 'absent',
 66
 'no diastema'
 'diastema present',
 67
 'single-rooted unicuspid lower canine'
 cusp of c1', 'accessory cusps are present on either side of the major
 68
 'large, raised above premolars'
 'small, about as high as premolars',
 69
 'no diastema'
 'short, less than the length of P1'
 'long, more than the length of P1',
 70
 'P1 is shorter than P2'
 'P1 is as long as P2'
 'P1 is longer than P2',
 71
 'tall distinct cusp'
 'small remnant or no cusp',
 72
 'no diastema'
 'short, less than the length of p1'
 'long, more than the length of p1',
 73
 'central cusp is not inflated'
 'central cusp is inflated widening the tooth anteriorly',
 74
 'P3 almost twice as long as P2'
 'P2 shorter than P3'
 'P2 and P3 subequal length'

'P2 longer than P3'
 'P2 twice as long as P3',
 75 'no diastemata'
 'short, less than the length of p1'
 'long, more than the length of p1',
 76 'p1 is shorter than either p2 or p3'
 'p1 is as long as p2 or p3',
 77 'tall distinct cusp'
 'none or small remnant',
 78 'tall distinct cusp'
 'none or small remnant',
 79 'no diastemata'
 'short, less than the length of p1'
 'long, more than the length of p1',
 80 'p3 almost twice as long as p2'
 'p2 shorter than p3'
 'p2 and p3 subequal length'
 'p2 longer than P3',
 81 'tall distinct cusp'
 'none or small remnant',
 82 'p3 major cusp laterally compressed'
 'p3 major cusp very large',
 83 'the anterior and posterior roots of p3 are level'
 'the anterior root of p3 is more exposed than the
 posterior root, reclining p3 toward m1',
 84 'StA is large, with a long crest running
 anteroposteriorly'
 'StA is small, with a short or no crest running
 anteroposteriorly'
 'StA remnant or no StA',
 85 'no StC or StB'
 'StB and StC are distinct cusps'
 'StB and StC are fused and oval in shape connected by a
 stylar crest but clearly identifiable as separate cusp'
 'StB and StC are fused and oval in shape connected by a
 stylar crest but difficult to clearly identify each cusp',
 86 'StB larger than StC'
 'StB subequal to StC'
 'StC larger than StB',
 87

88 'StB/C and StD are connected by a series of crests'
 'StB/C and StD are not connected by any crests',
 'absent'
 'present'
 'present and wide',

89 'postprotocrista ends on anterior flank of metacone'
 'postprotocrista ends on lingual flank of metacone'
 'postprotocrista ends on posterolingual flank of metacone'
 'postprotocrista joins with the posterior cingulum and ends posteriorly to the midpoint of the postmetacrista'
 'postprotocrista joins with the posterior cingulum and ends at the lingual flank of the metastylar tip',

90 'metaconule is directly positioned at the base of the metacone'
 'a small shelf is between the base of the metacone and the metaconule'
 'a larger shelf is between the base of the metacone and the metaconule',

91 'present'
 'absent',

92 'StE present as a distinct cusp'
 'remnant of StE as a stylar crest or small cusp'
 'no StE (no stylar crest)',

93 'no anterior cingulum'
 'small anterior cingulum lingual to anterior tip of tooth'
 'small anterior cingulum connected to protocone shelf by a small shelf'
 'large anterior cingulum expanded further up to the protocone',

94 'StA is large, with a long crest running anteroposteriorly'
 'StA is small, with a short or no crest running anteroposteriorly'
 'no StA',

95 'StB is oval with a stylar crest running through it'
 'StB is conical with no stylar crest connection',

96 'StB and StD are connected by a series of crests'
 'StB and StD are not connected by any crests',

97 'preparacrasta terminates at base of StB (no crest connection).'

'preparacrista terminates at the tip StB'
 'preparacrista connects to StB with a weak connection to
 StA'
 'preparacrista connects to parastylar tip/StA',
 98
 'stylar crest present on St D connects to metastylar tip'
 'StD is a conical cusp not connected to the stylar crest
 running to the metastylar tip'
 'StD is a conical cusp and no stylar crest present',
 99
 'absent'
 'present'
 'present and wide',
 100
 'postprotocrista ends on anterior flank of metacone'
 'postprotocrista ends on lingual flank of metacone'
 'postprotocrista ends on posterolingual flank of metacone
 ,
 'postprotocrista joins with the posterior cingulum and
 ends posteriorly to the midpoint of the postmetacrista'
 'postprotocrista joins with the posterior cingulum and
 ends at the lingual flank of the metastylar tip',
 101
 'metaconule is directly positioned at the base of the
 metacone'
 'a small shelf is between the base of the metacone and the
 metaconule'
 'a larger shelf is between the base of the metacone and
 the metaconule',
 102
 'Present as tall cusp'
 'small remnant present'
 'absent',
 103
 'present'
 'absent',
 104
 'StE present as a distinct cusp'
 'remnant of StE as a stylar crest'
 'no StE (no stylar crest)',
 105
 'StA is large, with a long crest running
 anteroposteriorly'
 'StA is small, with a short or no crest running
 anteroposteriorly'
 'no StA',
 106
 'StB is oval with a stylar crest running through it'
 'StB is conical with no stylar crest connection (except by
 wear)',
 107
 'StB and StD are connected by a series of crests'

108 'StB and StD are not connected by any crests',
 'preparacrista terminates at base of StB (no crest
 connection)'
 'preparacrista terminates at the tip StB. '
 'preparacrista connects a crest linking StA and StB'
 'preparacrista connects to parastylar tip/StA',
 109 'stylar crest present on StD connects to metastylar tip'
 'StD is a conical cusp not connected to the stylar crest
 running to the metastylar tip'
 'StD is a conical cusp and no stylar crest present',
 110 'postprotocrista ends on anterior flank of metacone'
 'postprotocrista ends on lingual flank of metacone'
 'postprotocrista ends on posterolingual flank of
 metacone'
 'postprotocrista joins with the posterior cingulum and
 ends posteriorly to the midpoint of the postmetacrista'
 'postprotocrista joins with the posterior cingulum and
 ends at the lingual flank of the metastylar tip',
 111 'metaconule is directly positioned at the base of the
 metacone'
 'a small shelf is between the base of the metacone and the
 metaconule'
 'a larger shelf is between the base of the metacone and
 the metaconule',
 112 'present as tall cusp'
 'small remnant present'
 'absent',
 113 'present'
 'absent',
 114 'StE present as a distinct cusp'
 'remnant of StE as a stylar crest'
 'no StE (no stylar crest)',
 115 'no anterior cingulum'
 'small anterior cingulum lingual to anterior tip of
 tooth'
 'small anterior cingulum connected to protocone shelf by
 a small shelf'
 'large anterior cingulum expanded further up to the
 protocone',
 116 'no StB'
 'small StB'
 'large StB',
 117

'no connection'
 'crest connecting the two cusps',
 118 'preparacrista terminates StA'
 'preparacrista terminates at the anterior flank of StB',
 119 'postparacrista straight'
 'postparacrista curves as a small centrocrista and ends
 just after the centrocrista',
 120 'postprotocrista ends anterior to the most posterior end
 of the postparacrista'
 'postprotocrista ends level with the most posterior end
 of the postparacrista'
 'postprotocrista ends posterior to the most posterior end
 of the postparacrista',
 121 'absent'
 'small metacone raise above the postparacrista'
 'large metacone expands the length of the tooth',
 122 'absent'
 'present',
 123 'present'
 'absent',
 124 'absent or small remnant'
 'present',
 125 'absent'
 'present',
 126 'paraconid-metaconid distance is longer than metaconid-
 protoconid distance'
 'paraconid-metaconid distance is as long as metaconid-
 protoconid distance'
 'paraconid-metaconid distance is shorter than metaconid-
 protoconid distance'
 'paraconid highly reduced or absent',
 127 'paraconid anterior to metaconid'
 'paraconid anterobuccal to metaconid',
 128 'oval'
 'triangular (wider posteriorly than anteriorly)'
 'conical',
 129 'cristid obliqua terminates buccal to level with the
 protocone'
 'cristid obliqua terminates lingual to the protocone to
 the midpoint to the tooth width'

the tooth width',
 130 'cristid obliqua terminates lingual to the midpoint of
 'oblique to the tooth row axis'
 'perpendicular to the tooth row axis',
 131 'posthypocristid connects to hypoconulid'
 'posthypocristid connects to base of entoconid when the
 tooth is unworn, but as the tooth wears down, a crest connects the tip of
 the entoconid to the posthypocristid',
 132 'large distinct cusp'
 'small cusp',
 133 'paraconid-metaconid distance is longer than metaconid-
 protoconid distance'
 'paraconid-metaconid distance is as long as metaconid-
 protoconid distance'
 'paraconid-metaconid distance is shorter than metaconid-
 protoconid distance'
 'paraconid highly reduced or absent',
 134 'cristid obliqua terminates buccal to the protocone'
 'cristid obliqua terminates lingual to the protocone
 about midpoint to the tooth width'
 'cristid obliqua terminates lingual to the midpoint of
 the tooth width',
 135 'oblique to the tooth row axis'
 'perpendicular to the tooth row axisp ',
 136 'posthypocristid connects to hypoconulid'
 'posthypocristid connects to entoconid',
 137 'large distinct cusp'
 'small cusp'
 'hypoconulid absent',
 138 'paraconid-metaconid distance is longer than metaconid-
 protoconid distance'
 'paraconid-metaconid distance is as longer as metaconid-
 protoconid distance'
 'paraconid-metaconid distance is shorter than metaconid-
 protoconid distance'
 'paraconid highly reduced or absent',
 139 'cristid obliqua terminates buccal to the protocone'
 'cristid obliqua terminates lingual to the protocone
 about midpoint to the tooth width'
 'cristid obliqua terminates lingual to the midpoint of
 the tooth width',
 140

'oblique to the tooth row axis'
 'perpendicular to the tooth row axis',
 141 'posthypocristid connects to hypoconulid'
 'posthypocristid connects to entoconid',
 142 'large distinct cusp'
 'small cusp'
 'hypoconulid absent',
 143 'paraconid-metaconid distance is longer than metaconid-
 protoconid distance'
 'paraconid-metaconid distance is as longer as metaconid-
 protoconid distance'
 'paraconid-metaconid distance is shorter than metaconid-
 protoconid distance'
 'paraconid highly reduced or absent',
 144 'present'
 'absent',
 145 'anteroposterior'
 'oblique',
 146 'absent'
 'present',
 147 'anteroposterior'
 'oblique',
 148 'cristid obliqua terminates lingual to the protocone
 about midpoint to the tooth width'
 'cristid obliqua terminates lingual to the midpoint of
 the tooth width',
 149 'oblique to the tooth row axis'
 'perpendicular to the tooth row axis '
 'anteriorly orientated',
 150 'large distinct cusp'
 'small cusp'
 'entoconid absent',
 151 'large distinct cusp'
 'small cusp'
 'hypoconulid absent',
 152 'buccal shelf end at buccal side of hypoconid'
 'buccal shelf buccally reduced (hypoconid more buccal
 than shelf)',
 153 'present'

154 'absent',
 'present'
 'Absent',
 155 'absent'
 'present',
 156 'absent'
 'present',

;
 MATRIX

```

'D. murgonensis'      ???0002100 11?1000000 ??????????
?????????00 ?????????? ?1011????? ?00????????? ???-103 1000120010
1110000001 101100000? ?011211011 2101100000 0001000110 001000-000 0100??
'M. archibaldi'      1-?0102100 00?0000001 0001020?0?
00001????20 101?210??1 211021????? ?00?????10 1101000002 1000100010
1111000001 1010101101 0010110011 100????00?? ????????110 001000-000 010000
'B. wangala'        1--0201100 00?1000000 0001020001
0000022120 211?210101 2100210010 0000??0010 0201001113 10000-0010
1211001001 0010101101 001110-011 2001000000 0000000010 000000-000 010000
'D. hallucatus'     1----021-0 ?00-000002 0001020000
0000022220 301?200201 ---0210010 0000000000 010-01000- ---20--010
1112011001 0111201021 0212110000 0000000000 0001000010 000000-002 111110
'D. byrnei'         1--0011100 ?01-000002 0001020001
0000012220 3010000101 00-0210000 1000001000 000401000- ---20-1110
1112011101 0211201111 021110-000 0001100000 0000011010 112000-001 210110
'P. tapoatafa'      1--0002201 ?011000002 0000020002
0000022220 2010010101 2000210000 0000000001 0002010103 1002100130
0122011013 0101200103 0211210000 0001100000 0001000010 000000-002 210000
'A. stuartii'       1--0012201 ?011000001 0000020002
0000022220 1010010201 2000210000 1000001000 0001011103 1001101130
1122011013 0111201123 0111210000 000(01)100000 0000000010 000000-001
110000
'S. macroura'       1--0001100 ?011000001 0000020011
0000013222 3010000201 2010210000 1000001000 0001010003 10000-1020
1111011002 0211201121 011110-000 00001000-0 0010000211 002000-001 210010
'C. ecaudatus'      00022200(02)0 22211-0011 1111122112
11(01)1113123 21010?1111 2021200(01)00 1101101121 0203000013 0000121011
1100113201 0211011320 0212010010 1000120210 0022000220 002000-100 200011
'M. lagotis'        0010120320 22211-1112 1111122010
(01)11?233333 3101(02)?1211 2021101101 0011110022 1103211113 100210100-
1230110200 -112211020 -112320112 0010130200 0031000310 0031-0-122 200010
'M. leucura'        0101220120 2221??0112 1111122010
11????33333 310?0?1211 2021001101 0011110022 0103211113 100110100-
1220110200 -212111020 -212220101 0010120201 0031100311 0021-0-122 200010
'I. australis'      ??????????? ???????101? ???????????
????????????? ??????????? ????1?0????? ?0?????????? ??????0110? ???????????
????????????? ??????????? ????????????? ????0120201 0031000??? ??????????? ??????
'P. broadbenti'     0111312220 (12)120000011 1111112210
00?01?0010 000?2?1110 2021000111 0001110120 0100100110 1000310011
0120011201 0200011321 021220-011 2000001000 0011000110 000000-100 200000
    
```


'P. raffrayana' 0112102130 2220000011 1110111210
0011100000 0001001110 1021000101 0001110120 0101101111 0000311021
0110012002 1201001321 1102111000 000(01)000000 0021000211 000000-100
200000

'M. longicauda' 0111000130 2220000012 1121111110
1001100010 0001001111 1001101001 1001110121 0101200013 1000311021
0110012102 1211011321 1212010000 1000000000 0011000211 0111-0-111 200000

'M. papuensis' 0111000130 2221000012 1121111110
10????00?? ?00?0?1?11 2001101001 0001111121 0203200023 1000311010
1110113001 1211011321 1212010010 1000000000 0011000210 0011-0-110
2000(01)0

'R. prattorum' 1--1202120 2220000011 1121101(12)11
00?111111? 000(01)001111 2021001(01)01 1001110120 0102201021 1000221021
0020113201 1202001321 1100010011 2000000000 0011000110 0001-0-100 100000

'E. clara' 1--1301130 ?220000012 1111112110
00?1101010 010?(02)?1111 2021101011 0001110020 1200201010 1100211010
1110011201 1202001221 1102211011 1000000000 0111001110 0101-0-101 100000

'E. davidi' 1--1201130 2220000011 11?111111?
00???0??1? 0?0?0?1111 20210010?1 1001110120 0201201111 0100311021
0110011202 1200011322 1110210001 1000000110 0111001210 0100010100 200000

'E. kalubu' 1--2102230 2220000012 1111111110
0001(12)01010 0101001111 2021001001 1001110120 0102201011 0000221021
0110013102 1101011312 1000210011 1000010110 0021000210 0101-0-101 200000

'E. rufescens' 1--1112230 2220000012 1111111210
00??201010 010?0?1111 2021001001 1001110120 0201201011 0000321021
0110013002 1201011322 1001(12)10011 210(01)000100 0021000210 0000111110
100000

'cf. P. tedfordi' ?????01120 22??00001? ??????????
???????????? ??????????? ????100???? ?00???????? ??????????? 00?0321010
0110011101 1101011311 1211???????? ????0100010 0011000110 00????????? ???????

'cf. P. sp.' ?????01?2? 2???00001? ???????????
???????????? ??????????? ????100???? ?00???????? ??????????? ???0321010
01????????? ??????????? ??????????? ????0100000 00??????211 10????????? ???????

'I. auratus' 0112212312 2221??1111 1120121111
10??223242 310?0?1111 2021001001 0101111011 0112110013 0101221242
1020113124 2210011324 2212320011 1000121211 0021100211 012010-010 200010

'I. obesulus' 0112212312 2220011111 1111121111
(01)0??223242 310?(01)?1111 2021001001 010111(01)011 011211001(23)
0101221242 1020113124 2210011324 2212320011 (12)00(01)121211 0021100211
112010-010 2000(01)0

'I. macrourus' 0113222322 2220(01)11111 1111121111
(01)01?223242 3101201111 2021001001 01011110(12)1 0111110011 0101221242
1020113224 2210011324 2210320011 2100121201 0021100211 112010-000
2000(01)0

'P. nasuta' 0112112021 2220??1011 1120121212
01?1112121 110?(01)?1211 2021001001 0001111011 010120001(23) 0000321232
0100113112 22(01)0011322 2212010011 2(01)00110200 0021101211 1121-0-110
2100(01)0

'P. bougainville' 0111112020 2221??0012 1120122212
11??213121 210?0?1(12)11 2021001001 0001111021 0102210013 0000221022
1100113102 2211011321 2210010010 1000110200 0021101211 0121-0-111 200010

```

      'P. gunnii'                0122222020 22211-0011 1120122212
1111113121 1101001111 2021001001 1001111021 0102200012 0000221022
1200013202 22(01)0011321 2210020000 2100110200 1021110211 1021-0-100
210010
      'P. eremiana'             01?1112030 2221??0012 1120122212
10?1113121 110?0?1111 2021001001 000111?021 0202210013 0000211022
1100113102 2211011321 2212010010 1000110200 0021101211 0121-0-11? 200010
      'P. sobbei'               ???????0?0 22?0??0012 ??????????
??????????? ???????1?? ??2110???? ?00???????? ?????2??013 000????????
??10113102 ?211011321 0212??????? ???0110201 1121111211 1121-0-111 20?0??
      'P. bowensis'            ???22??1?0 22??01001? ???????????
??????????? ??????????? ?0?100???? ?00???????? ???????????? 0??????????
??10113202 221?011321 0212??????? ???0100210 00?????211 11????????? ??????
      'P. allinghamensis'      ??????????? 2?????????? ???????????
??????????? ??????????? ??????????? ?0????????? ??????????? ???????????
??20113202 221????????? ??????????? ??????????? ??????????? ??????????? ??????
      'Y. burchfieldi'          ???1002120 11201-0012 ?100111000
1?100????21 000?2??11?1 ?02120?10? 000?1000?? ???001002 1010320010
1110003001 0111000311 021110-000 0001100200 0000000010 0011-0-112 200000
      'Y. kida'                  ??????02120 11??000012 ???????????
??????????? ??????????? ???120???? ?00???????? ??????????? ???0321010
1110003001 0111000321 0211110000 0001100000 0000000010 0011-0-112 20????
      'G. speciosus'            00?1202210 (12)2?0000011 0101111000
00100???11 100?2??11?1 202100000? 000???0000 0101001101 1110310131
1120003002 1211010322 1211210000 0000100010 0011000210 002000-110 200000
      'G. grandis'              ??????02201 11??000011 ???????????
??????????? ???????1?? ??2110???? ?00???00?? ???101111 1110320131
1120003013 1211000322 1201??????? ???0100010 0011000110 000000-100 10?0??
      'G. amplus'               ???1202210 22??000011 ?101111???
10????????? ??0?2??1?1 ?02100?0?? 000???0010 ?2??101111 1110320131
1120013002 1211011322 121020-000 0001111010 0021100211 0021-0-110 200000
      'G. adversus'             ??????02210 21????????? ???11?1???
??????????? ??????????? ??????????? ?00???????? ??????????? ???0310110
1120013011 0211011321 0211210000 000????????? ??????????? ??????????? ??????
      'B. palara'               ???1001120 (12)221000011 ?1001?1000
10?00?1121 100?0?1(12)?? 2021(01)0??0? 0?0?1000?0 1101101003 00102(02)0011
011000(13)001 1101001321 11121(01)0000 100(01)100(01)00 0021000211
(01)01000-010 200000
      'B. muirheadae'           ??????01110 11??000011 ???????????
??????????? ??????????? ???100???? ?00????????? ??????????? ???0221010
0110010001 0101001311 0110??????? ???1100000 0020000211 0010010000 10????
      'B. campbelli'           ???????1?0 ?2??000011 ???????????
??????????? ??????????? ???100???? ?00????????? ??????????? ???????????
??????????? ???001321 111????????? ???11?0(01)00 0?21000211 0010010100
10?????

```

;

ENDBLOCK;

BEGIN ASSUMPTIONS;

OPTIONS DEFTYPE=UNORD POLYTCOUNT=MINSTEPS;

TYPESET * default = ORD: 4 - 13 20 23 26 - 28 30 35 - 37 39 45 48 51
53 55 69 - 72 74 - 75 79 - 80 84 86 88 - 90 92 - 94 97 - 102 104 - 105 108
- 112 114 - 116 120 - 121 126 129 133 - 134 137 - 139 142 - 143 149 - 151;

ENDBLOCK;

APPENDIX 3

Topology enforced in our molecular scaffold analysis (based on Krajewski et al., 2007; Westerman et al., 2008, 2012):

